Supplementary Materials

Include

Supplementary Methods and References

Supplementary Figures and Legends

Supplementary Tables

Supplementary Methods

Human subjects and primary renal PTC lines

Self-reported African Americans undergoing nephrectomy for localized renal cell carcinoma with a preoperative eGFR >60 ml/min per 1.73 m^2 were consented to provide non-diseased kidney tissue, blood and urine. Fifty individuals (male/female 26:24; mean±SD age, 58.3±10.9 years; and serum creatinine 1.06±0.33 mg/dl) were enrolled between March 2010 and May 2015 and the study was approved by the Wake Forest School of Medicine (WFSM) Institutional Review Board. Participants provided written informed consent. Primary renal PTC lines were established from kidney tissue using an established protocol.[1]

DNA was isolated from peripheral blood using Promega DNA isolation wizard kits (Promega, Madison, WI). Two SNPs in the *APOL1* G1 kidney-risk allele (rs73885319; rs60910145) and an insertion/deletion for the G2 kidney-risk allele (rs71785313) were genotyped using a custom assay designed at WFSM on the Sequenom platform (Sequenom Laboratories, San Diego, California).[2] G1 and G2 genotype calls were visually inspected for quality control. Genotyping efficiency was 100% and 41 blind duplicates resulted in a 100% concordance rate.

Global gene expression, identification of eQTLs and pathway analysis

Global gene expression profiles were performed on primary renal PTCs from African Americans (with and without poly IC) using Affymetrix HTA 2.0 arrays.[3] The Illumina Multi-Ethnic Genotyping Array (MEGA) chip was used to genotype SNPs throughout the genome.[3]

Total RNAs were isolated from 50 non-diseased primary renal PTC line samples from African Americans before and after treatment with 2.5 ug/ml poly IC for 16 hours. RNAs were processed on Affymetrix HTA2.0 arrays to determine levels of relative global gene expression. The Affymetrix arrays were done in a single batch. The quality control analysis and normalization process confirmed the absence of failed samples or outliers. Whole genome transcript intensity profiles were extracted using Transcriptome Analysis Console (TAC) software for Affymetrix HTA 2.0 arrays. Levels of expression

were estimated based on RMA4 normalized log2 converted probe set pixel intensity. The threshold for detectable transcripts was set at a signal/noise ratio >3. Gene expression data from Affymetrix HTA 2.0 arrays are available in the NCBI Gene Expression Omnibus (GEO) database.

For genotype data, standard quality control measures (i.e. 95% call rate thresholds, gender checks, heterozygosity, relatedness) for GWAS analyses were completed. Admixture estimates were computed using the program, ADMIXTURE.[4] These estimates were used to confirm self-reported ancestry and one admixture estimate (African ancestral proportion) was included as a covariate in association analyses.

To test for associations between SNPs and mRNA expression levels, a linear regression was computed which adjusted for admixture as a covariate. These tests were computed using QSNPGWA version 4.0 module of SNPLASH (https://www.phs.wakehealth.edu/public/bios/gene/downloads.cfm). Using *APOL1* mRNA expression as the outcome, this method was computed genome-wide to capture both cis- and trans- SNPs associated with *APOL1* mRNA expression. To evaluate effects of *APOL1* KRVs on global transcriptome levels, SNP-mRNA associations were computed using the *APOL1* KRVs, coded as an additive (0 vs. 1 vs. 2) or recessive (0/1 vs. 2) model, with each mRNA transcript meeting QC as the outcome. Information from the top eQTLs was used to explore the likeliest pathways linking *APOL1* with cellular dysfunction.

Paired analysis between primary PTCs before and after poly IC exposure was performed for differentially expressed genes by empirical Bayers method[5] implemented in R Biocondoctor limma package. The selection thresholds |logFC| >1 and FDR (False Discovery rate) $p<0.01$ were used. Cytoscape (http://www.cytoscape.org/) and Ingenuity Pathway Analysis (IPA) (http://www.ingenuity.com/) were performed to identify significant pathways relevant to poly IC.

Knockout of BAK1 in the human podocyte cell line

The human podocyte cell line[6] was used to generate BAK1 knockout cells. BAK1 CRISPR/Cas9 KO plasmid (Cat # sc-400646) and BAK1 HDR plasmid (Cat # sc-400646-HDR) were obtained from Santa Cruz BioTech. Cell transfection was performed following the manufacture's instruction using UltraCruz® transfection reagent (sc-395739, Santa Cruz) and plasmid transfection medium (sc-108062, Santa Cruz). A

puromycin resistance sequence was introduced. Cells were selected with RPMI-1640 (Cat # 11875-093, Thermo Fisher Gibco) containing 10% FBS (Cat # F7524, Sigma-Aldrich) supplemented with TSI (Cat # I-3146, Sigma-Aldrich) and 0.25μg/ml puromycin (sc-108071, Santa Cruz) 24h post-transfection. Selection medium was replaced every 48h for 28 days. Individual clones were isolated, expanded, and maintained in RPMI-1640 media with 10% FBS, TSI and 0.25μg/ml puromycin. Six clones were characterized. Individual clones were verified by immunoblotting and immunofluorescence to determine APOL1 protein expression levels in wild type and KO cell lines.

Establishment of HEK293 Tet-on APOL1 G0, G1, G2 and EV cells

HEK293 Tet-on *APOL1* cell lines were established to stably express G0, G1, G2 and empty pTRE2hyg vector (EV) based on previously reported methods.[7] Briefly, cDNAs of *APOL1* G0, G1, and G2 were inserted into the NheI- and SalI-digested pTRE2hyg vector (Clontech, Mountain View, CA). To obtain Tet-inducible cell lines stably expressing *APOL1*, HEK 293 Tet-On 3G cell lines (Clontech, Mountain View, CA) were transfected in 100 mm dishes at 30% confluence with 5 μg pTRE2hyg plasmid containing *APOL1* G0, G1, G2, and empty vector using Lipofectamine transfection reagent (Invitrogen, Waltham, MA) based on manufacturer instructions. Cells were selected with DMEM (Invitrogen) containing 10% FBS supplemented with 400 μg/ml G418 (Cellgro, Manassas, VA) and 100 ug/ml hygromycin B (Invitrogen, Waltham, MA) 24 h post-transfection. Selection medium was replaced every 48h for 20 days. Individual clones were isolated, expanded, and maintained in DMEM media with 10% FBS, 100 μg/ml G418 and 50 ug/ml hygromycin B (referred to as complete DMEM growth media). Eight clones were characterized for each variant; one clone per variant was selected for all experiments. Individual clones were verified by direct sequencing (ABI 3730XL, Applied Biosystems, Foster City, CA) and immunoblotting was used to determine *APOL1* expression levels and APOL1 protein size. Individual clones with G0, G1 and G2 *APOL1* genotypes and empty pTRE2hyg vector were analyzed for inducible *APOL1* expression by RT-PCR, immunoblot analysis, and immunofluorescence.

Immortalized human kidney cell lines

Conditionally immortalized human proximal tubule and podocyte cell lines were cultured in basic growth medium as described previously.[1] Material transfer agreements were signed and approved by all involved institutional review boards.

Total RNA isolation, quality control, and real-time PCR

Total RNA was isolated from HEK293 Tet-on cells using RNAeasy Mini Kit (Qiagen, Germany). The quantity and quality of isolated RNA were determined by ultraviolet spectrophotometry and electrophoresis, respectively, on the Nanodrop 2000 (Thermo Fisher Scientific, Wilmington, DE) and Agilent 2100 Bioanalyzer (Agilent Technologies, Santa Clara, CA). To determine *APOL1* mRNA levels in cells, 200ng of RNA was reverse transcribed with random hexamer primers using the TaqMan RT kit (Applied Biosystems, Foster City, CA). Primers were designed to capture all known *APOL1* splice variants. RT-PCR in the presence of SYBRGreen was performed with a Roche 480 Real-Time PCR system (Roche Diagnostics, Germany) using 18S ribosomal RNA or β-actin for normalization. Primer sequences were described in Supplementary Table S3. The ΔΔCT method[8] was used to quantify the relative levels of *APOL1* mRNA. Fold-changes were normalized to mRNA levels on HEK293 Tet-on G0 cells without Dox induction. All experiments were performed in triplicate and results expressed as mean ± SD if not specified.

Immunoblotting

Immunoblotting was performed as described previously.[9] Blots were incubated overnight at 4°C with primary antibodies (Supplementary Table S4). The membranes were then washed four times in Tris-buffered saline containing 0.1% Tween 20 and incubated for 1 hour in blocking buffer with anti-mouse/rabbit IgG conjugated to horseradish peroxidase (1:20,000; Jackson ImmunoResearch Laboratories).

Fluorescence Microscopy

Immunofluorescence of APOL1 (Epitomics, Burlingame, CA) and mitochondrial marker ATP5A1 (Invitrogen, Frederick, MD) and other markers was performed on HEK293 Tet-on cell lines using established protocols.[1] Information for primary antibodies is summarized in Supplementary Table S4. Secondary antibodies (goat anti-rabbit Alexa Fluor 594 or 680 and goat anti-mouse Alexa Fluor 488, Jackson ImmunoResearch Laboratories) were used to display fluorescent signals (1:100 dilution). Fifty nM

of mitotracker Green (Invitrogen) and 10 nM of TMRE (Invitrogen) were incubated with HEK293 Tet-on cells for 30 minutes prior to signal detection. Microscopy was performed using an Olympus IX71 fluorescence microscope (Olympus Scientific Solutions Americas Corp., Waltham, Massachusetts).

Assessment of mitochondrial morphology

Mitochondrial morphology was captured by mitotracker Red (Invitrogen) using a confocal microscope (Olympus FV1200) with CO2 concentration maintained at 5% and temperature at 37 °C in a controlled chamber. Z-stack was applied to generate clearly focused mitochondrial images for subsequent morphological evaluation on randomly selected fields. Areas of 100μm x 100μm were imaged with a 100x oil objective lens.

Mitochondrial elongation and fragmentation were estimated by grouping cells into elongated, intermediate, and fragmented categories using similar methods as Karbowski *et al.*[10] Briefly, "elongated" cells were those with >75% of mitochondria forming elongated interconnected network, "intermediate" with mixed tubular and short mitochondria, and "fragmented" with >75% short punctiform mitochondria. At least 100 cells were imaged for each genotypic/treatment group of live primary proximal tubule cell lines (PTCs) and HEK293 Tet-on cell lines from multiple image fields (6/genotype/independent experiment). Two independent cell culture experiments per primary PTC line and three independent cell culture experiments for HEK293 Tet on cell lines were performed to allow comparison for rate of mitochondrial elongation or fragmentation among PTCs of different *APOL1* genotypes with/without poly IC treatment and among HEK293 Tet-on cells of different *APOL1* genotypes with Dox(-)/(+) or Mdivi-1 treatment, respectively.

Live cells were imaged on a confocal microscope at 1000x. Mitochondrial integrity was assessed with Mitotracker Red. Mitochondrial length was scored as mean length of rods and branches in μm using Fiji, a distribution of the popular open source software Image J (https://imagej.nih.gov/ij/docs/guide/146-2.html), integrated with a plug-in macro toolset Mitochondrial Network Analysis (MiNA). MiNA is freely available at http://github.com/ScienceToolkit/MiNA. The tool incorporates optional preprocessing steps to enhance quality of images before converting the images to binary and produce a morphological skeleton to

quantitatively capture the morphology of mitochondrial network.[11] Image fields which contained 15-25 live cells were further chosen to measure mitochondrial length (rods/network branches). During image preprocessing in Fiji, "Subtract Background" was chosen with a radius of 50. Noise was set at "Despeckle". Enhance Local Contrast (CLAHE) was turned on with a combination of blocksize = 9 and slope = 4. To match the actual mitochondrial network pattern, "Tubeness" was set at default for HEK 293 Tet-on cells and "2" for primary tubule cells respectively according to the thickness of mitochondrial tubes.[12] The MiNA macro (version 2) was run under the default setting.

Cell viability assay

Stabilized HEK293 Tet-on *APOL1* G0, G1, G2 and empty vector cells (20,000/well) were seeded on three 96-well plates. After 24 hours of growth, cells were induced with doxycycline (Dox) for 24 or 16 hours in complete DMEM media; non-induced cells were also incubated with DMEM media but without Dox. Cell viability was measured using the Cytotox 96 lactate dehydrogenase (LDH) viability assay kit (Promega, Madison, WI) per manufacturer instructions. Each cell line (with and without Dox induction) was measured a minimum of six times, with values expressed as mean ± SD on bar graphs. Complete cell viability was defined as 1.0 (100% viable). The final concentrations of Mdivi-1 and Mito-Q for mitochondrial rescue testing were chosen based on prior optimized conditions.[13,14]

References

1. Ma L, Shelness GS, Snipes JA *et al.* Localization of APOL1 protein and mRNA in the human kidney: nondiseased tissue, primary cells, and immortalized cell lines. *J. Am. Soc. Nephrol. JASN* 2015; **26**: 339–348.
2. Freedman BI, Langefeld CD, Turner J *et al.* Association of APOL1 variants with mild kidney disease in first-degree relatives of African American patients with non-diabetic end stage renal disease. *Kidney Int* 2012; **82**: 805–811.
3. Ma L, Chou JW, Snipes JA *et al.* APOL1 Renal-Risk Variants Induce Mitochondrial Dysfunction. *J Am Soc Nephrol* 2017; **28**: 1093–1105.
4. Alexander DH, Novembre J, Lange K. Fast model-based estimation of ancestry in unrelated individuals. *Genome Res* 2009; **19**: 1655–1664.
5. Smyth GK. Linear models and empirical bayes methods for assessing differential expression in microarray experiments. *Stat. Appl. Genet. Mol. Biol.* 2004; **3**.
6. Saleem MA, O'Hare MJ, Reiser J *et al.* A conditionally immortalized human podocyte cell line demonstrating nephrin and podocin expression. *J. Am. Soc. Nephrol. JASN* 2002; **13**: 630–638.
7. Cheng D, Weckerle A, Yu Y *et al.* Biogenesis and cytotoxicity of APOL1 renal risk variant proteins in hepatocytes and hepatoma cells. *J. Lipid Res.* 2015; **56**: 1583–1593.
8. Livak KJ, Schmittgen TD. Analysis of relative gene expression data using real-time quantitative PCR and the 2(-Delta Delta C(T)) Method. *Methods* 2001; **25**: 402–408.
9. Ma L, Murea M, Snipes JA *et al.* An ACACB variant implicated in diabetic nephropathy associates with body mass index and gene expression in obese subjects. *PloS one* 2013; **8**: e56193.
10. Karbowski M, Norris KL, Cleland MM *et al.* Role of Bax and Bak in mitochondrial morphogenesis. *Nature* 2006; **443**: 658–662.
11. Valente AJ, Maddalena LA, Robb EL *et al.* A simple ImageJ macro tool for analyzing mitochondrial network morphology in mammalian cell culture. *Acta Histochem.* 2017; **119**: 315–326.
12. Strack S, Usachev YM eds. *Techniques to Investigate Mitochondrial Function in Neurons*. Springer New York; 2015.
13. Akita M, Suzuki-Karasaki M, Fujiwara K *et al.* Mitochondrial division inhibitor-1 induces mitochondrial hyperfusion and sensitizes human cancer cells to TRAIL-induced apoptosis. *Int. J. Oncol.* 2014; **45**: 1901–1912.
14. McManus MJ, Murphy MP, Franklin JL. The mitochondria-targeted antioxidant MitoQ prevents loss of spatial memory retention and early neuropathology in a transgenic mouse model of Alzheimer's disease. *J. Neurosci. Off. J. Soc. Neurosci.* 2011; **31**: 15703–15715.

Supplementary Figures

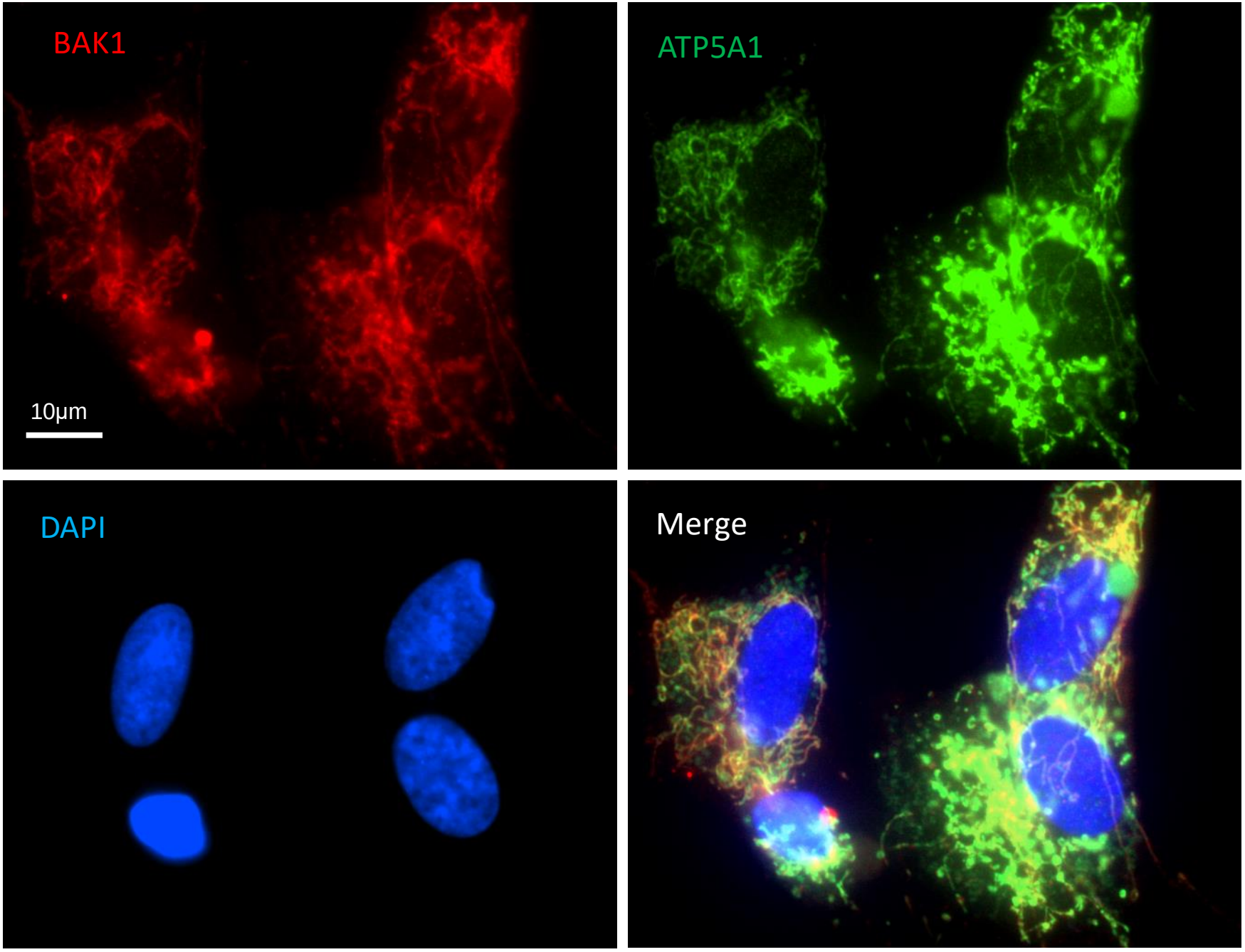

Supplementary Figure S1

Supplementary Figure S1. Presence of BAK1 protein in human renal proximal tubule cells (PTCs). Cultured human differentiated PTCs were washed with PBS and fixed with 4% paraformaldehyde. Cells were stained for BAK1 (red) with rabbit anti-BAK1 antibody (Cell Signaling), mitochondria (green) with ATP synthase 5 A1 (ATP5A1) antibody, and counterstained with nuclear dye 4',6-diamidino-2-phenylindole (DAPI; blue). BAK1 appeared to co-localize with mitochondria in renal PTCs.

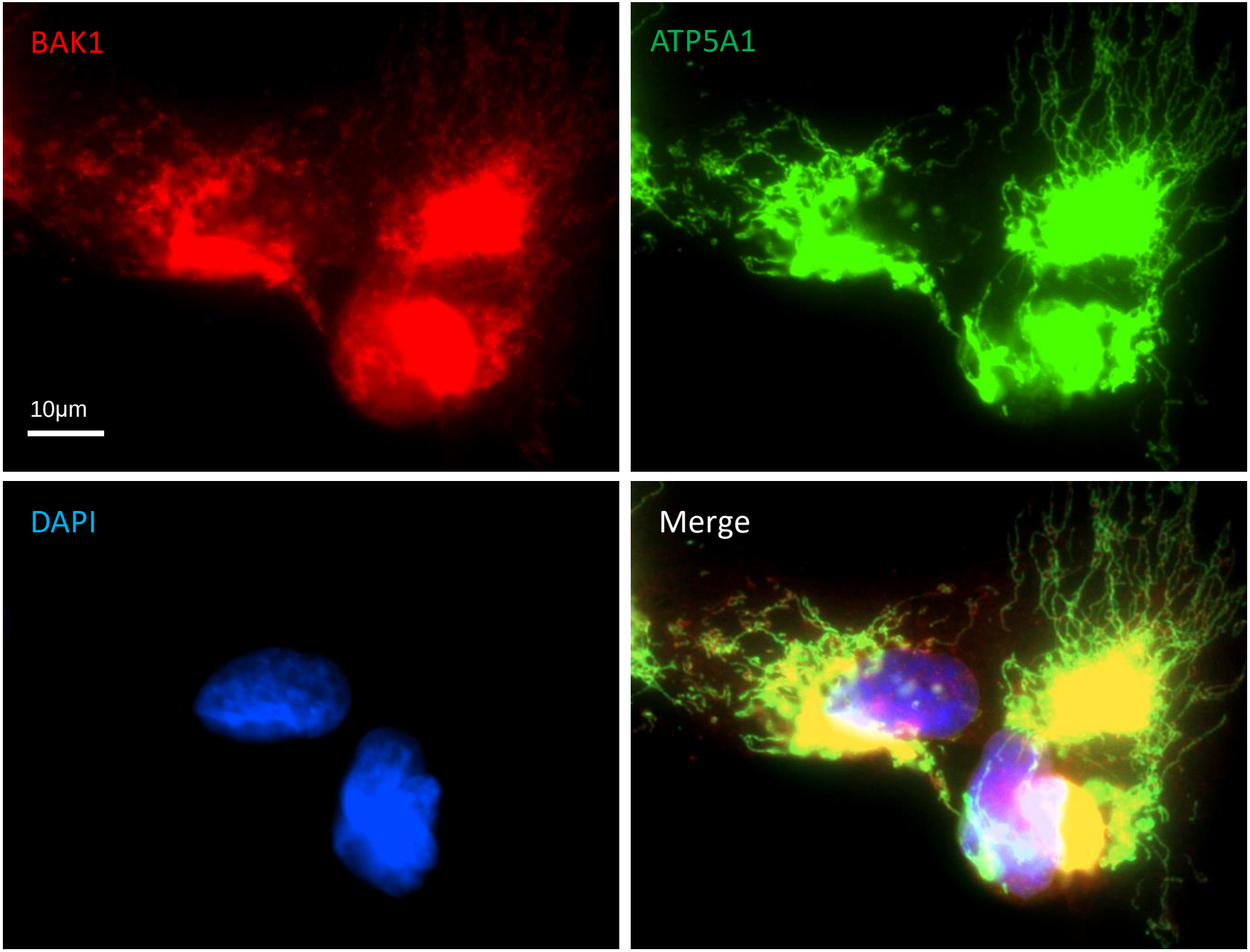

Supplementary Figure S2

Supplementary Figure S2. Presence of BAK1 protein in immortalized podocytes. Cultured human differentiated podocytes were washed with PBS and fixed with 4% paraformaldehyde. Cells were stained for BAK1 (red) with rabbit anti-BAK1 antibody (Cell Signaling), mitochondria (green) with ATP synthase 5 A1 (ATP5A1) antibody, and counterstained with nuclear dye 4',6-diamidino-2-phenylindole (DAPI; blue). BAK1 appeared to co-localize with mitochondria in immortalized human podocytes.

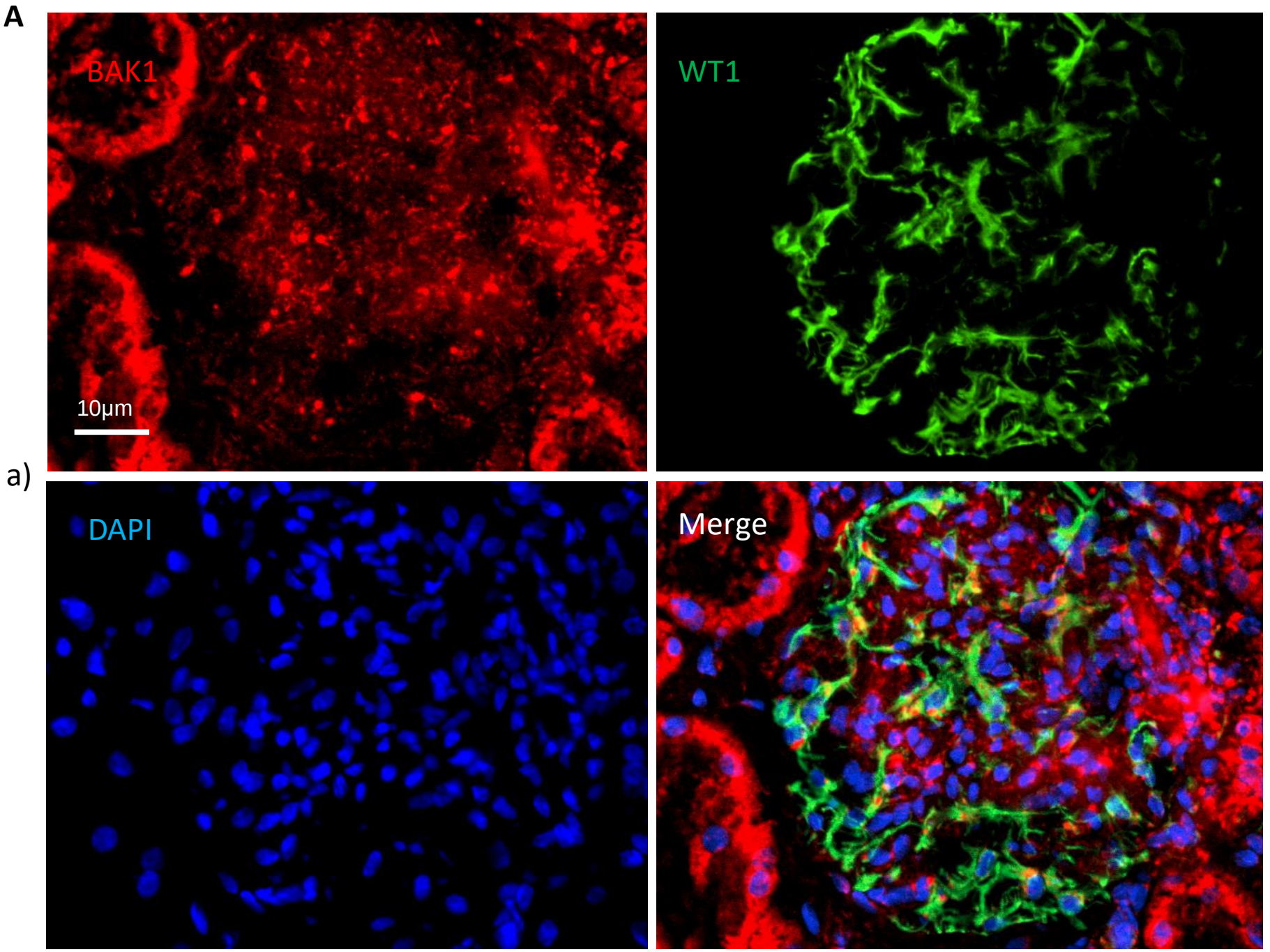

Supplementary Figure S3

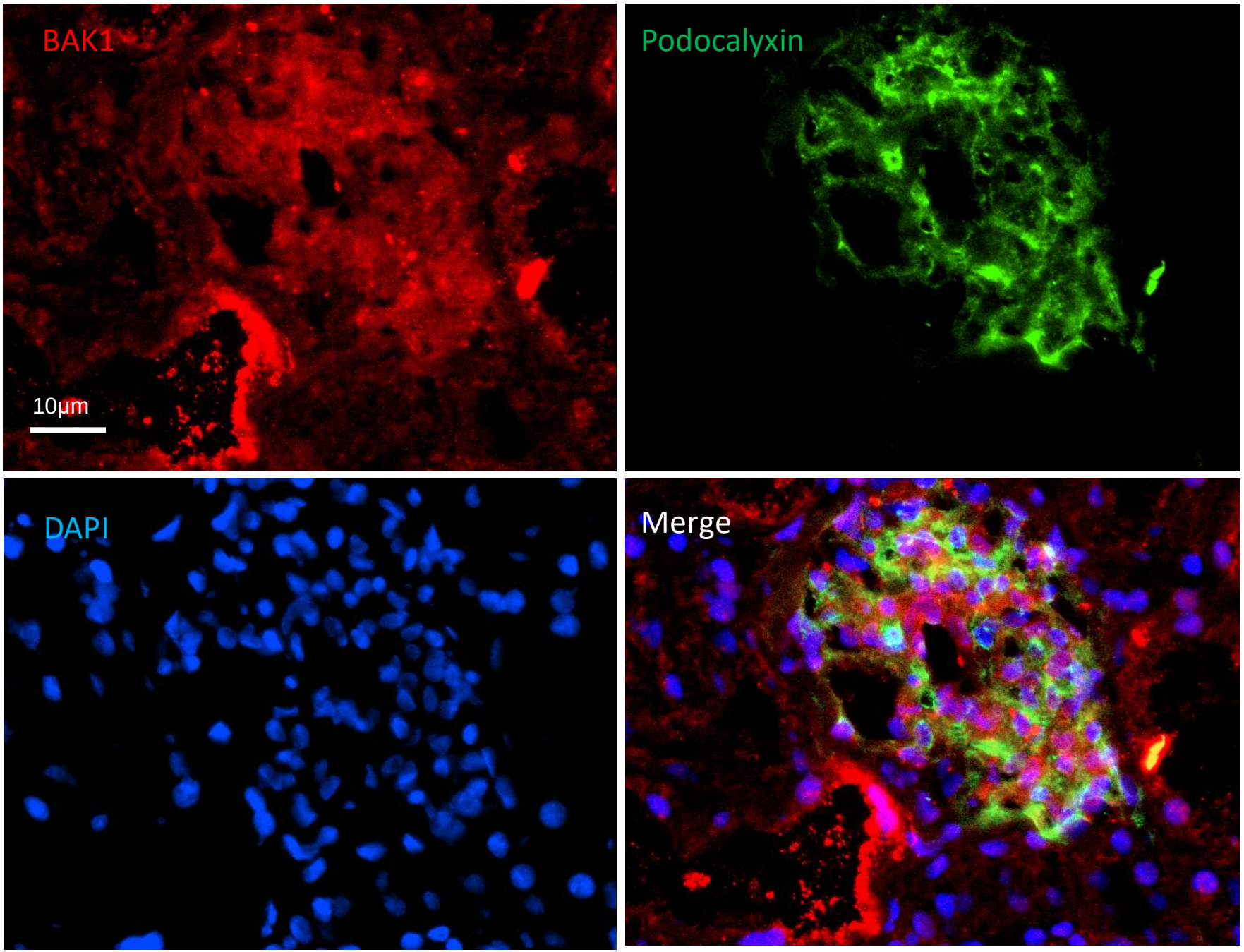

Supplementary Figure S3

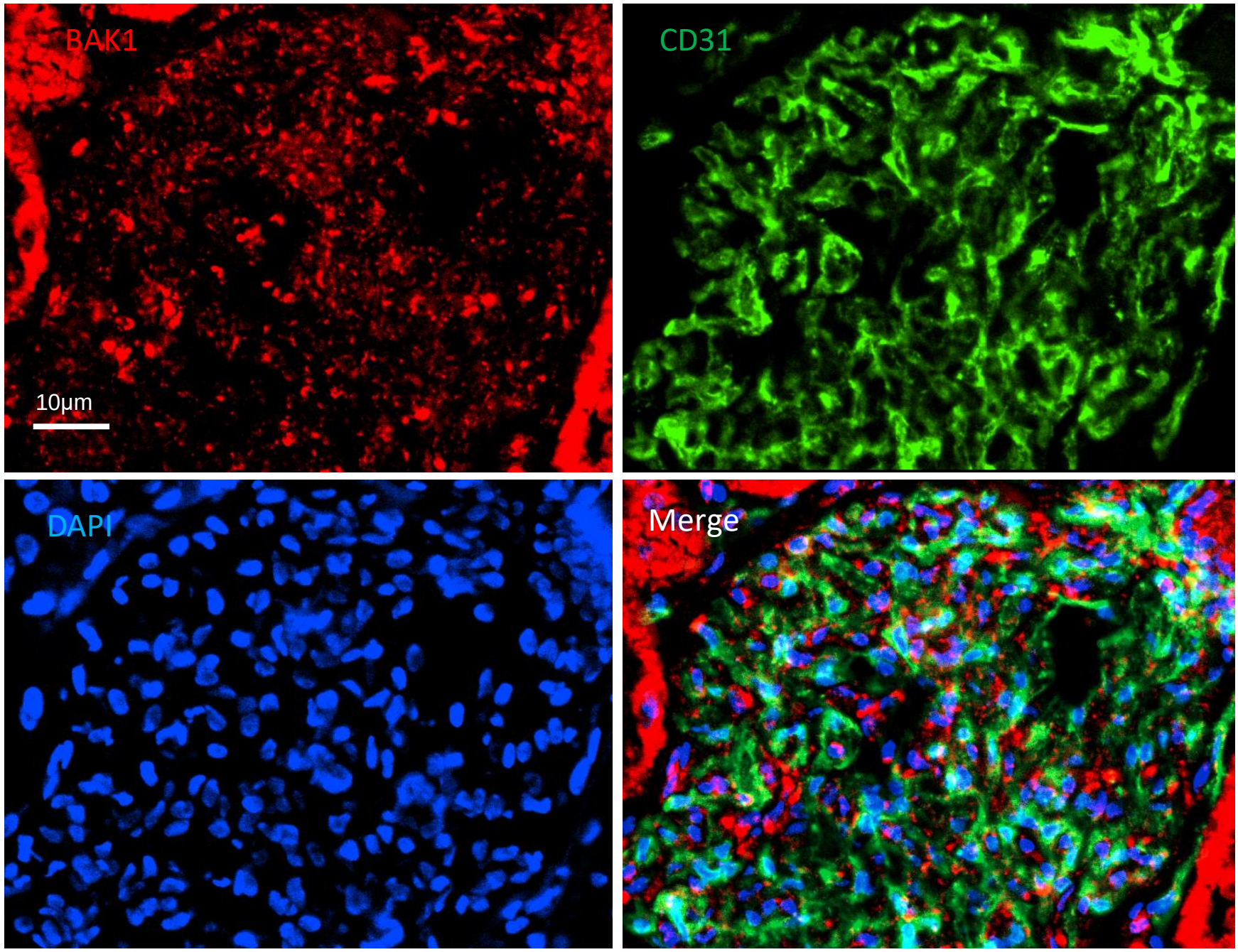

Supplementary Figure S3

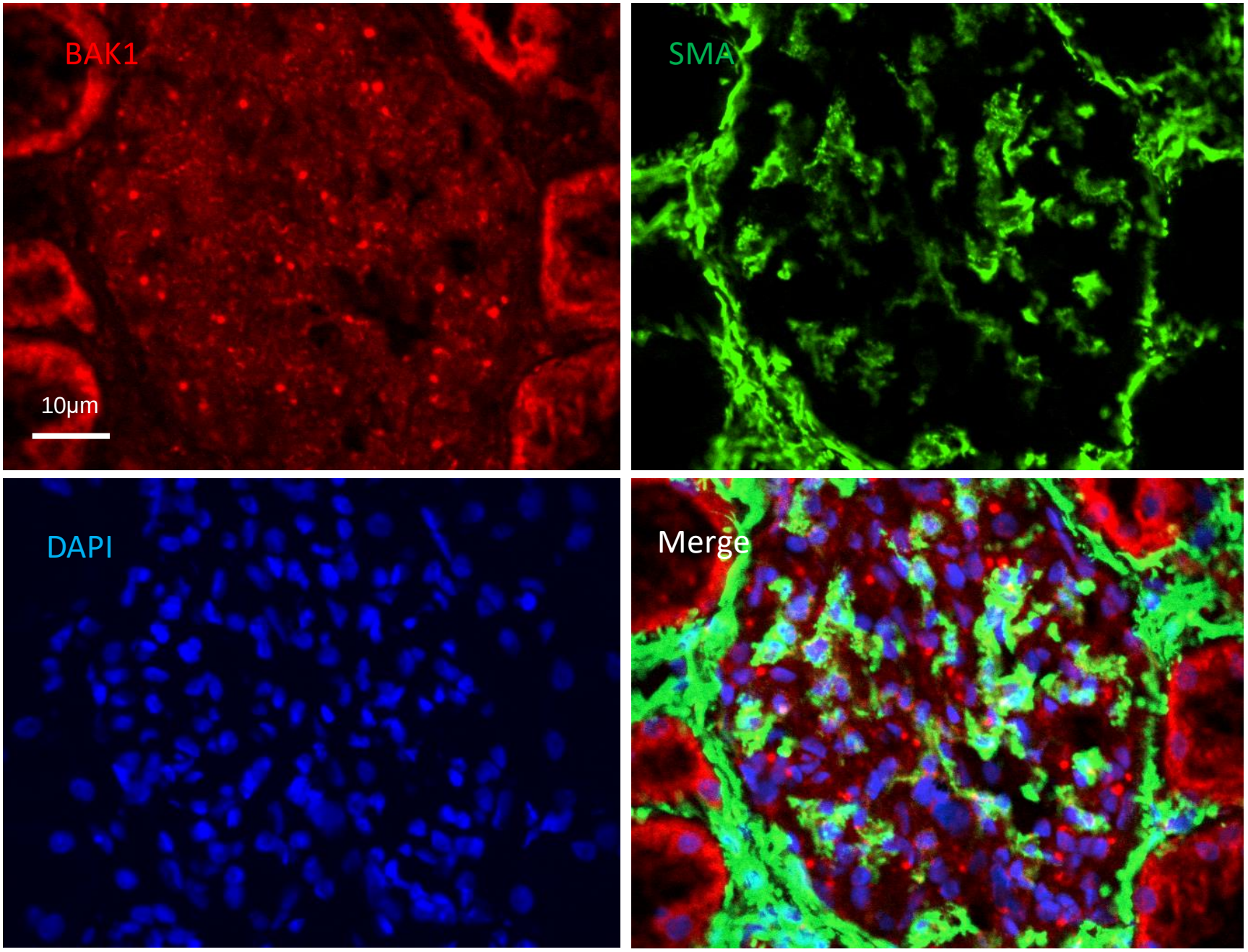

Supplementary Figure S3

D

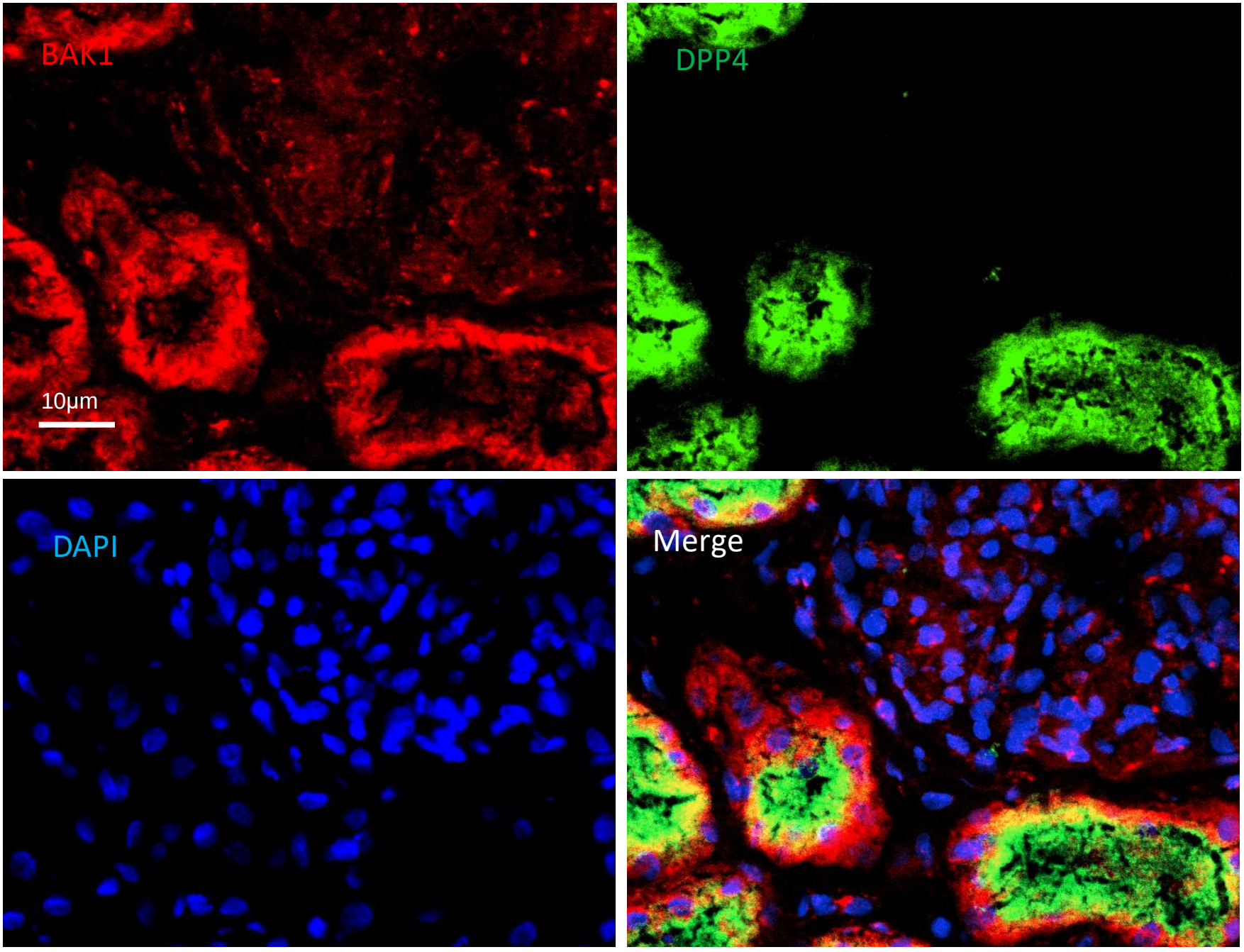

Supplementary Figure S3

E

Isotype controls

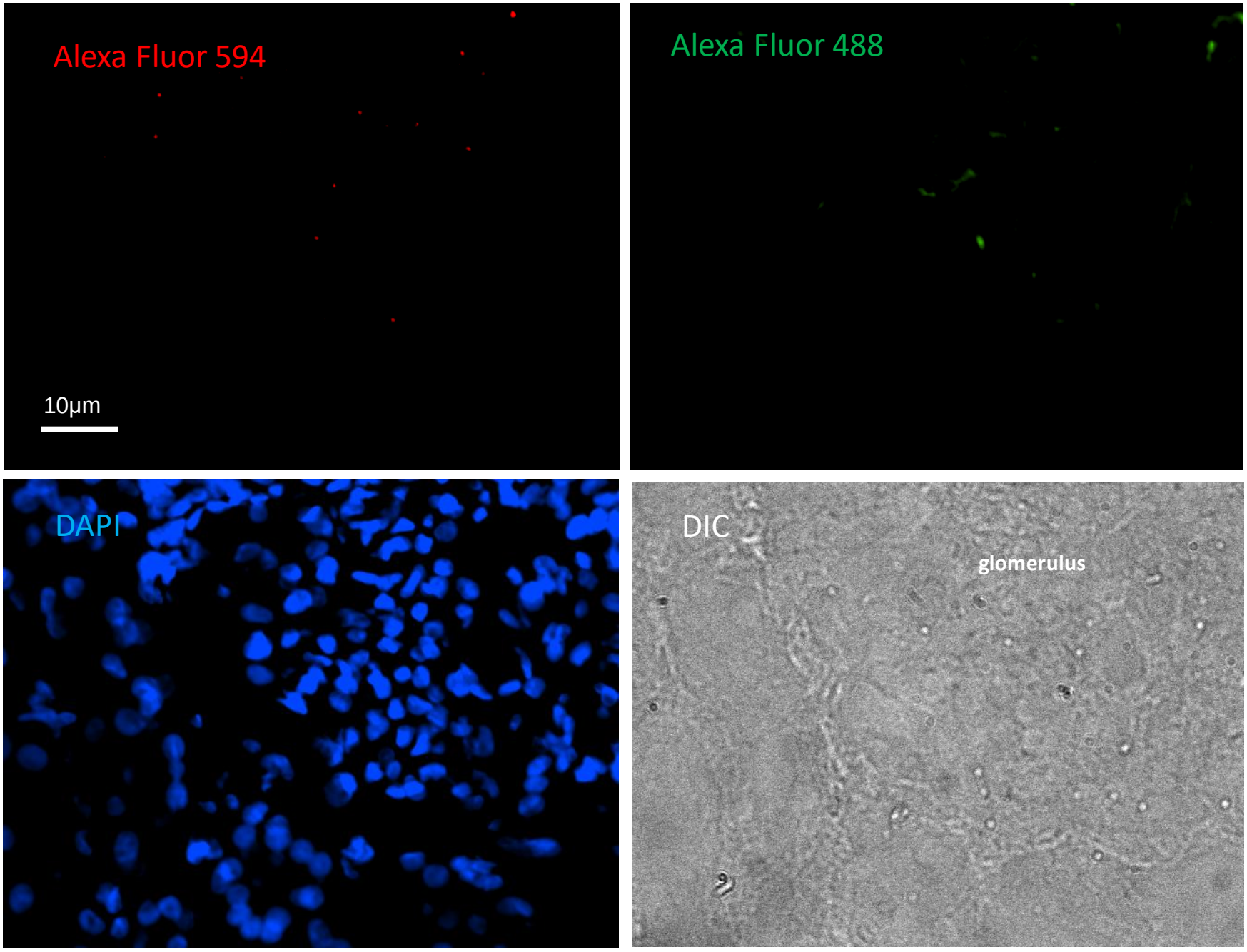

Supplementary Figure S3

Supplementary Figure S3. Presence of BAK1 on non-diseased human kidney cryosections. Immunofluorescence localization of BAK1 and A) WT1/Podocalyxin (podocyte markers), B) CD31 (endothelial cell marker), C) SMA (mesangial cell marker), D) DPP4 (renal proximal tubule cell marker) in non-diseased human kidney cryosections. Kidney cryosections were stained for BAK1 (red) and WT1/Podocalyxin/CD31/SMA/DPP4 (green), and counterstained with 4',6-diamidino-2-phenylindole (DAPI) (blue). BAK1 signals were enriched in tubules, with weaker expression in glomeruli. Overlay suggests BAK1 localizes in podocytes and proximal tubule cells. E) Diluted normal rabbit serum (1:200; Lampire Biological Laboratories, custom-made, Lot # 14C50017) and normal mouse serum (1:200; Jackson ImmunoResearch, Cat # 015-000-120, Lot # 135338) served as isotype controls for primary antibodies. Secondary antibodies (goat anti-rabbit Alexa Fluor 594 and goat anti-rabbit Alexa Fluor 488, Invitrogen) did not display meaningful fluorescent signals.

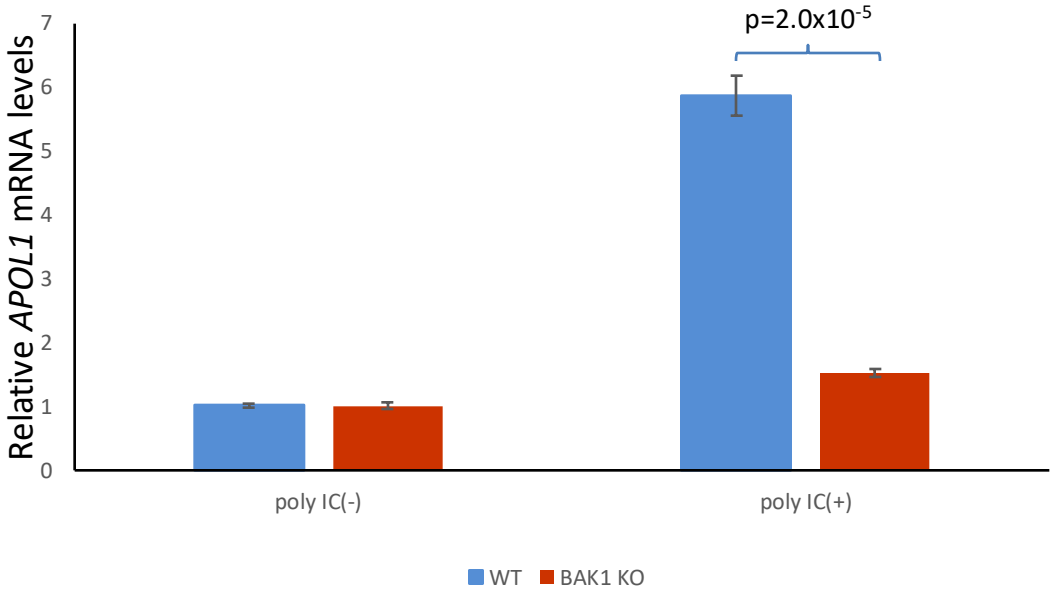

Supplementary Figure S4. *APOL1* messenger RNA level responses to the presence of poly IC and *BAK1* by RT-PCR. Podocyte cell lines (WT and BAK1 KO), treated without or with Poly IC (0.15ug/ml) for 16 hours, were washed with PBS and then lysed with RLT buffer (Qiagene) for RNA isolation. Without poly IC treatment, *BAK1* knockout did not inhibit *APOL1* messenger RNA levels. With poly IC treatment, *BAK1* knockout inhibited *APOL1* messenger RNA upregulation. Fold changes were normalized to mRNA levels of WT cells without poly IC treatment. *APOL1* mRNA levels in WT cells without poly IC treatment set at 1 (reference). RT-PCR was performed to assess the *APOL1* transcript levels; *ACTB* (β-actin) RNA was used as endogenous control for gene expression. Data are expressed as mean ± SD for triplicate experiments.

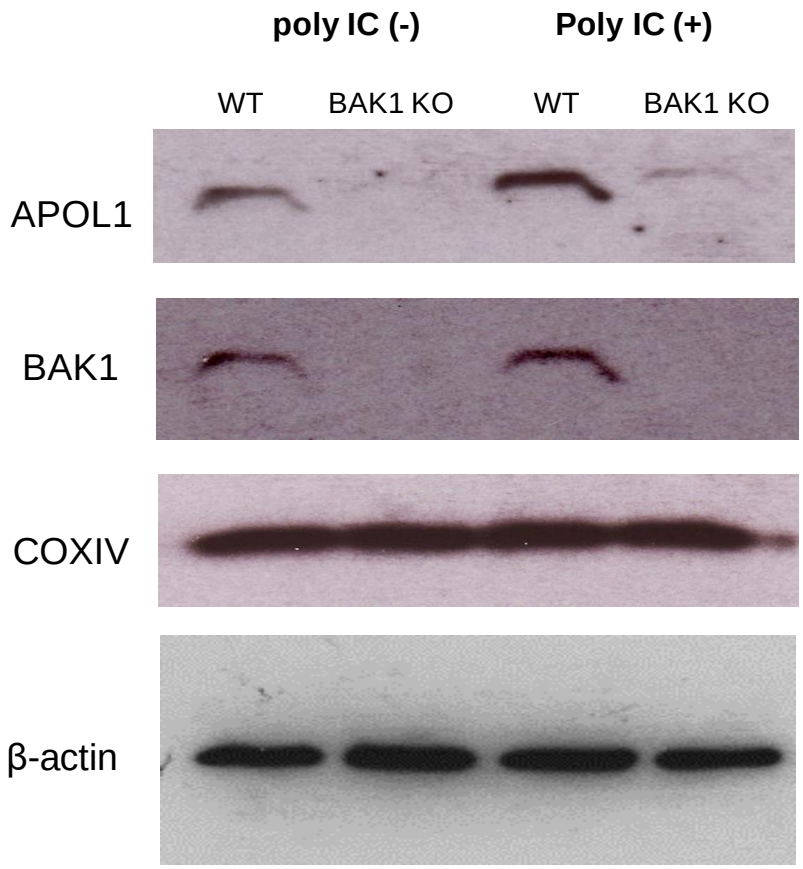

Supplementary Figure S5. APOL1 protein level responses to the presence of BAK1 by immunoblotting. Podocyte cell lines (WT and BAK1 KO), treated with or without Poly IC (0.15ug/ml) for 16 hours, were washed with PBS and then lysed with CHAPS buffer, heated in 6x loading buffer at 95^{o}C for 5 minutes reducing. Eight ug total protein was loaded onto a 4-20% SDS-PAGE gel and probed with APOL1 (Sigma), BAK1 (Santa Cruz), COXIV, and β-actin antibodies. BAK1 was undetectable in the BAK1 KO podocyte cell line with or without poly IC treatment; BAK1 level increased in the WT podocyte cell line after treatment with poly IC. APOL1 level significantly decreased in the BAK1 KO podocyte cell line with or without poly IC treatment; APOL1 significantly increased in the WT podocyte cell line after treatment with poly IC. COXIV (mitochondrial loading control) and β-actin were comparable among podocyte cell lines of WT and BAK1 KO, regardless of poly IC treatment. The data are representative of three trials of immunoblot with similar results.

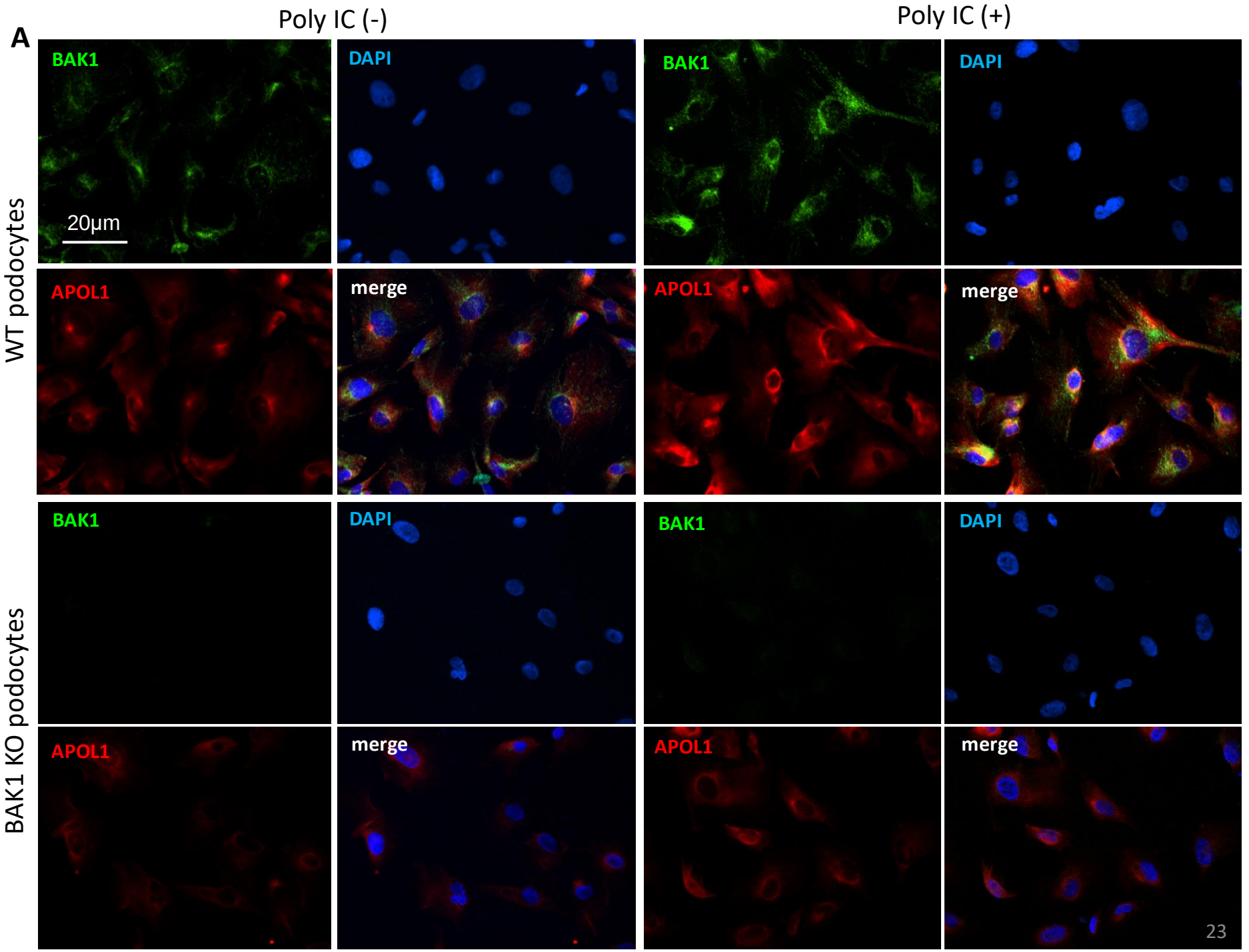
A
Poly IC (-)
Poly IC (+)
WT podocytes
BAK1 KO podocytes
BAK1
DAPI
APOL1
merge
20μm

B

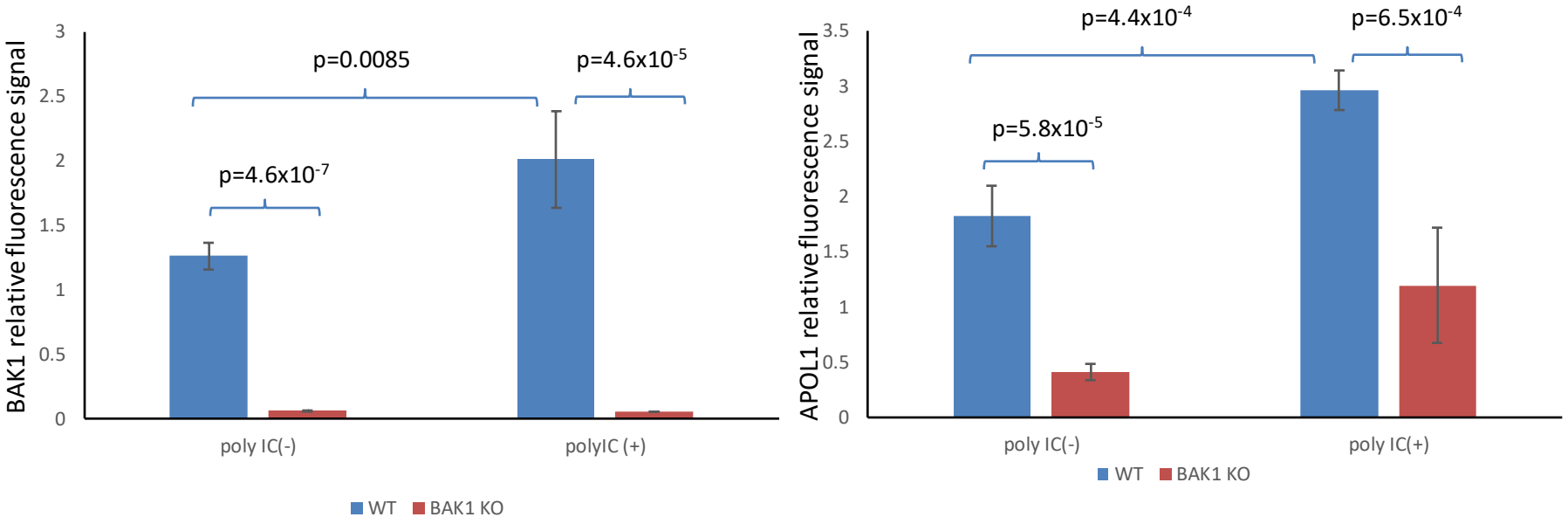

Supplementary Figure S6. APOL1 protein level responses to the presence of BAK1 by immunofluorescence.
A) Cultured human differentiated podocytes lines (WT and BAK1 KO), treated with or without Poly IC (0.15ug/ml) for 16 hours, were washed with PBS and fixed with 4% paraformaldehyde. Cells were stained for BAK1 (green) with mouse anti-BAK1 antibody (Santa Cruz), APOL1 (red) with rabbit anti-APOL1 antibody (Abcam), and counterstained with nuclear dye 4',6-diamidino-2-phenylindole (DAPI; blue).
B) BAK1 was almost undetectable in the BAK1 KO podocyte cell line with or without poly IC treatment; BAK1 level increased in the WT podocyte cell line after treatment with poly IC. APOL1 level significantly decreased in the BAK1 KO podocyte cell line with or without poly IC treatment; APOL1 significantly increased in the WT podocyte cell line after treatment with poly IC. The BAK1 and APOL1 signal intensities were normalized by DAPI in four independent wells of WT and BAK1 KO cells with and without poly IC treatment.

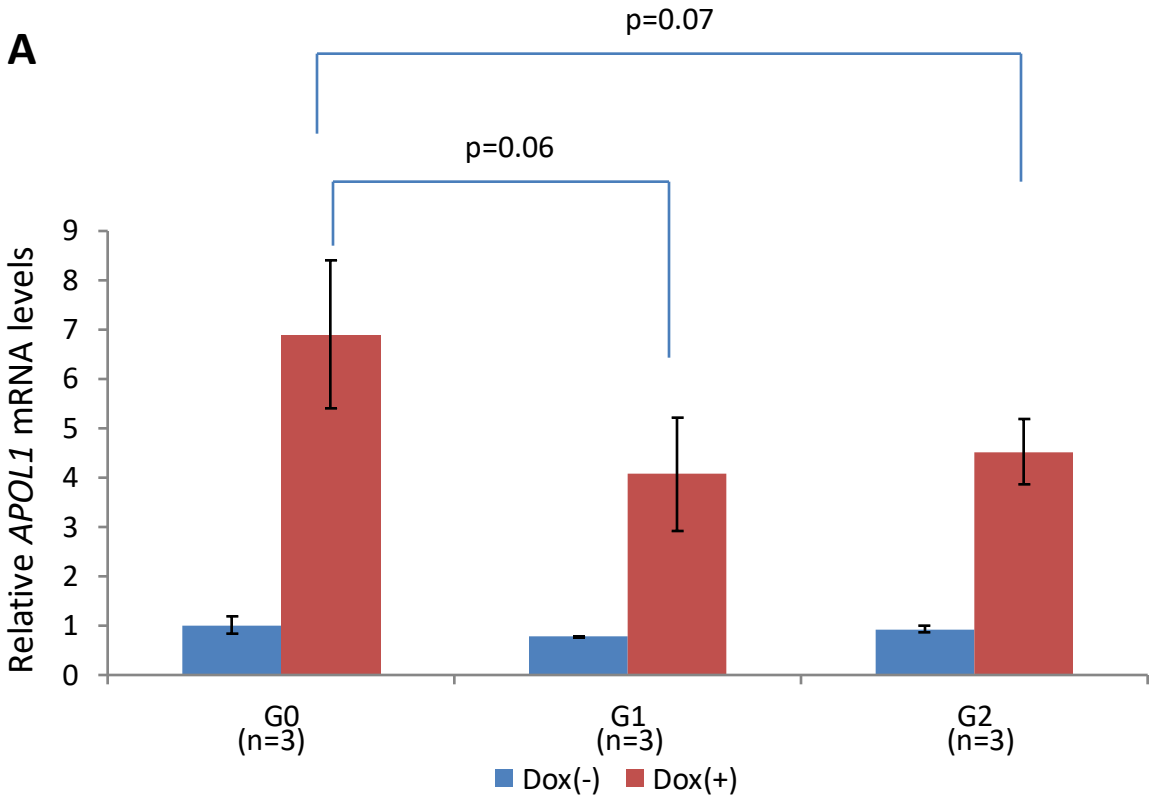

Supplementary Figure S7. Comparable of *APOL1* gene expression in HEK293 Tet-on cells.

A) Relative *APOL1* mRNA expression levels were comparable in HEK293 Tet-on G0, G1, and G2 cells with Dox (+) induction for 24 hr. HEK293 Tet-on cells without (-) or with (+) Dox induction were grown in complete DMEM growth media for 24 hr. Final Dox concentration for HEK293 Tet-on G0, G1, and G2 cells was 10ng/ml. RT-PCR was performed to assess the *APOL1* transcript levels; 18s RNA was used as endogenous control for gene expression. Fold changes were normalized to mRNA levels in non-induced G0 cells. Data are expressed as mean ± SD (n=3 independent experiments). *APOL1* mRNA levels in non-induced G0 cells were set at 1 (reference). Dox induced APOL1 G0 mRNA level was slightly higher than were G1 or G2 in corresponding HEK 293 Tet-on cells, however, the differences were not statistically significant.

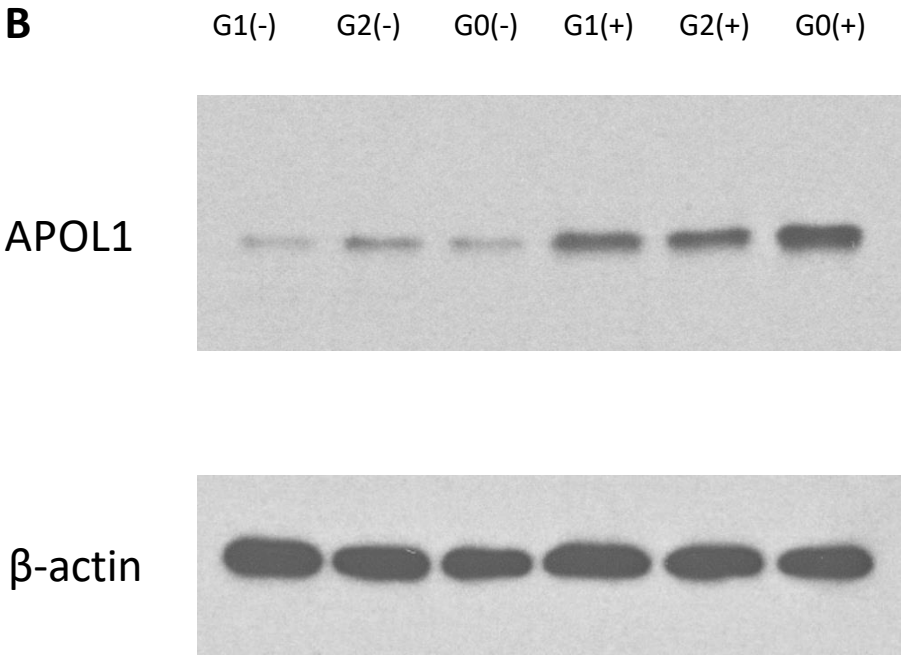

Supplementary Figure S7. Comparable *APOL1* gene expression in HEK293 Tet-on cells.
B) Relative APOL1 protein levels were comparable in HEK293 Tet-on cells of different genotypes with Dox induction for 24 hr. HEK293 Tet-on cells were induced with final Dox concentrations of 10ng/ml for HEK293 Tet-on G0, G1, and G2 cells in complete DMEM media for 24 hr. Four ug of total cell lysate protein was loaded onto a 4-20% SDS-PAGE gel and probed with APOL1 (Abcam) and β-actin antibodies. Dox-induced expression of APOL1 G0 was slightly higher than G1 and G2. Trace amounts of APOL1 were present in HEK293 Tet-on cells without Dox induction. The data are representative of three trials of immunoblot with similar results.

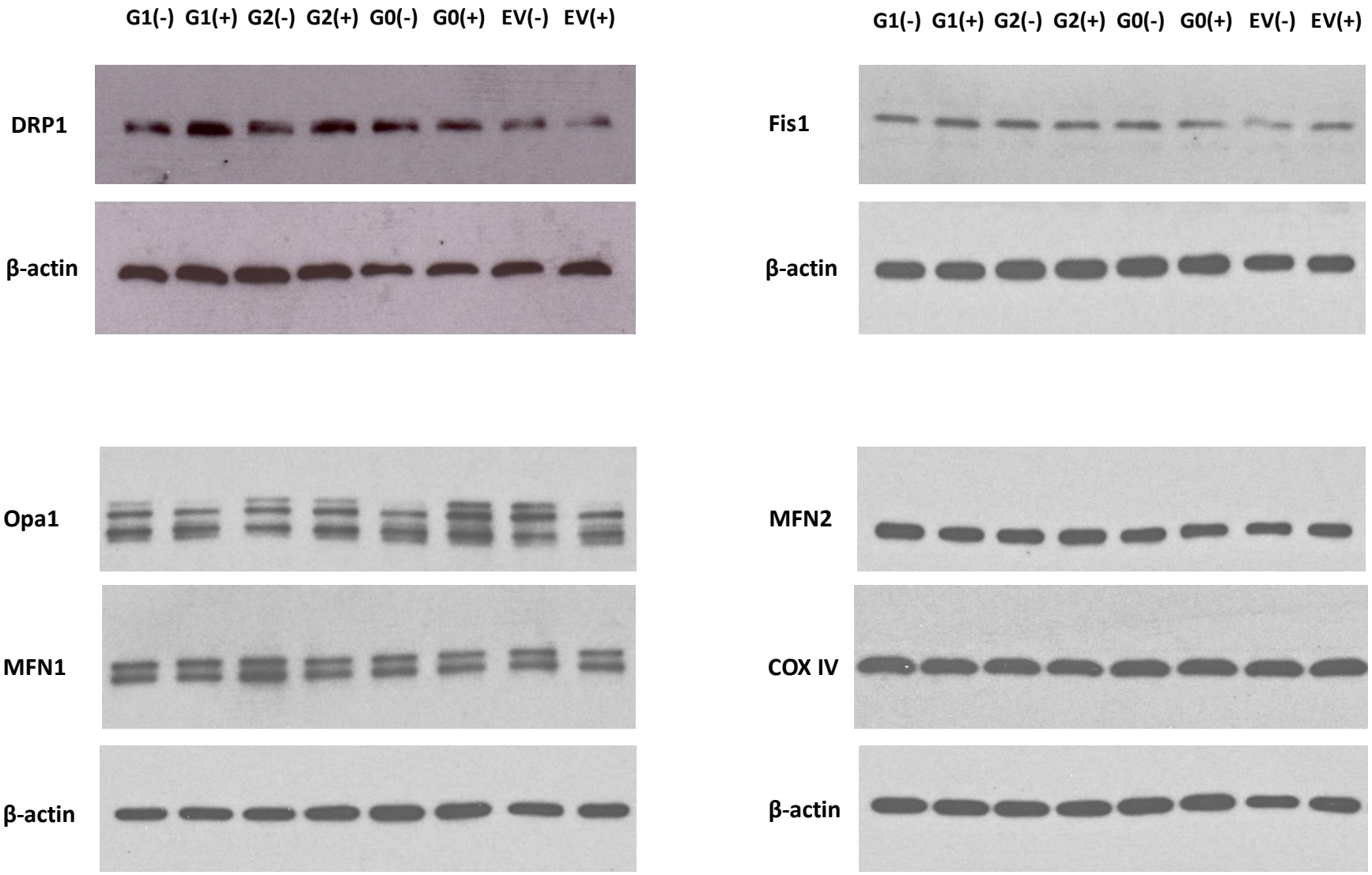

Supplementary Figure S8

Supplementary Figure S8. Mitochondrial fission marker DRP1 increased in HEK293 Tet-on G1 and G2 cell lines. HEK293 Tet-on cells with (+) or without (-) Dox induction were grown in complete DMEM growth media for 24 hr with final Dox concentration of 10ng/ml. Four ug of total cell lysate protein was loaded onto a 4-20% SDS-PAGE gel and probed with DRP1 (dynamin-1-like protein), Fis1 (mitochondrial fission 1 protein), Opa1 (mitochondrial dynamin like GTPase), MFN1 (mitofusin-1), MFN2 (mitofusin-2), COXIV (mitochondrial complex IV), and β-actin antibodies. HEK293 Tet-on empty pTRE2hyg vector cells (EV) were included to estimate non-specific background (without APOL1). Relative DRP1 protein levels (by β-actin) were increased in G1(+) and G2(+) cells, compared to G1(-) and G2(-) cells, respectively; relative DRP1 protein levels were decreased in G0 (+) cells compared to G0 (-) cells. As phospho-DRP1 is the active form of DRP1, additional assessment of p-DRP1 (Ser616) was performed on HEK293 Tet-on cells using immunofluorescence (see Supplementary Figure S9). Differences in Fis1, Opa1, MFN1, and MFN2 were not observed based on APOL1 genotype or Dox induction. COXIV (mitochondrial loading control) and β-actin were comparable among HEK293 Tet-on cells with or without Dox induction. Data are representative of three trials of immunoblot (with similar results in each).

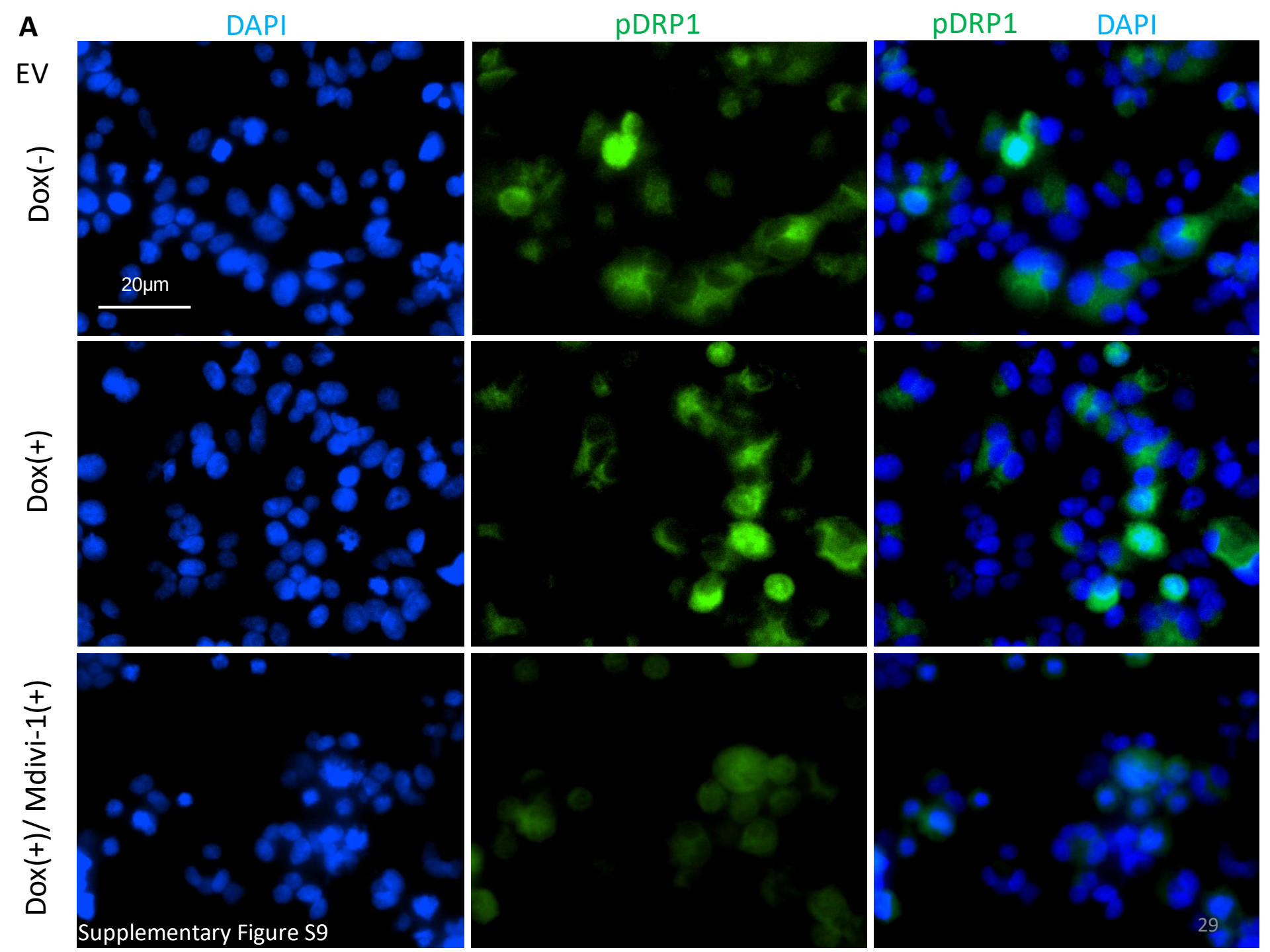

Supplementary Figure S9

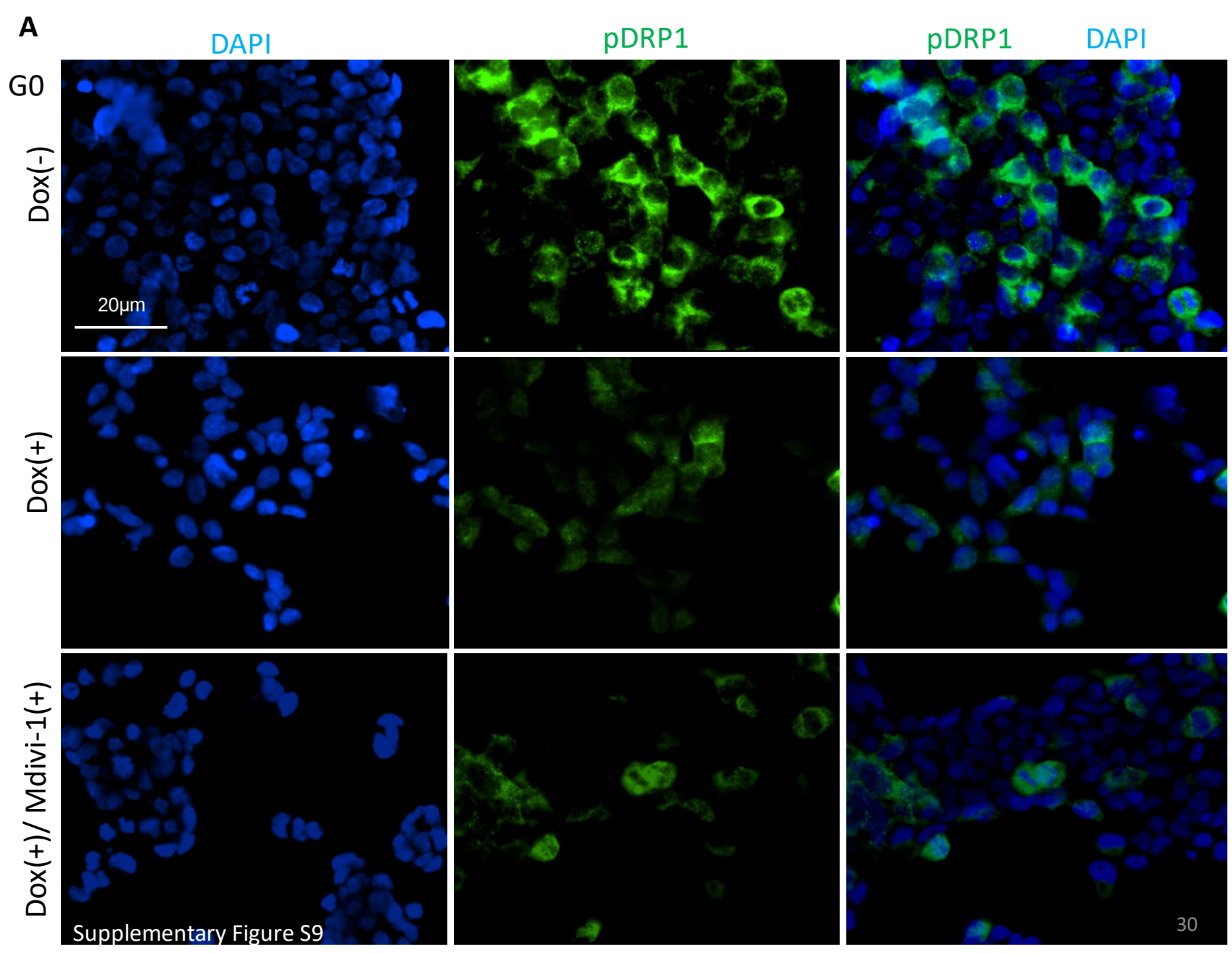

Supplementary Figure S9

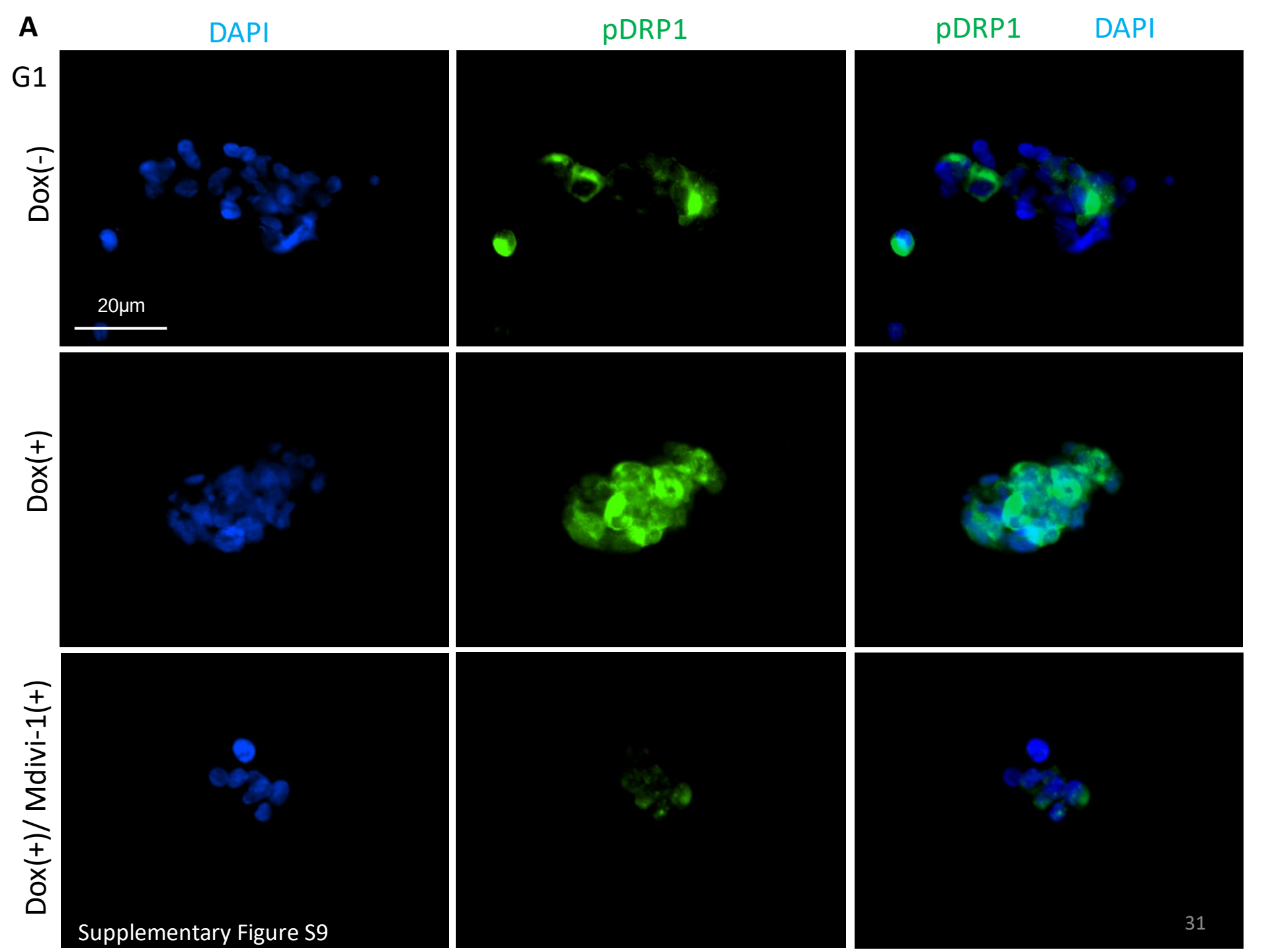

Supplementary Figure S9

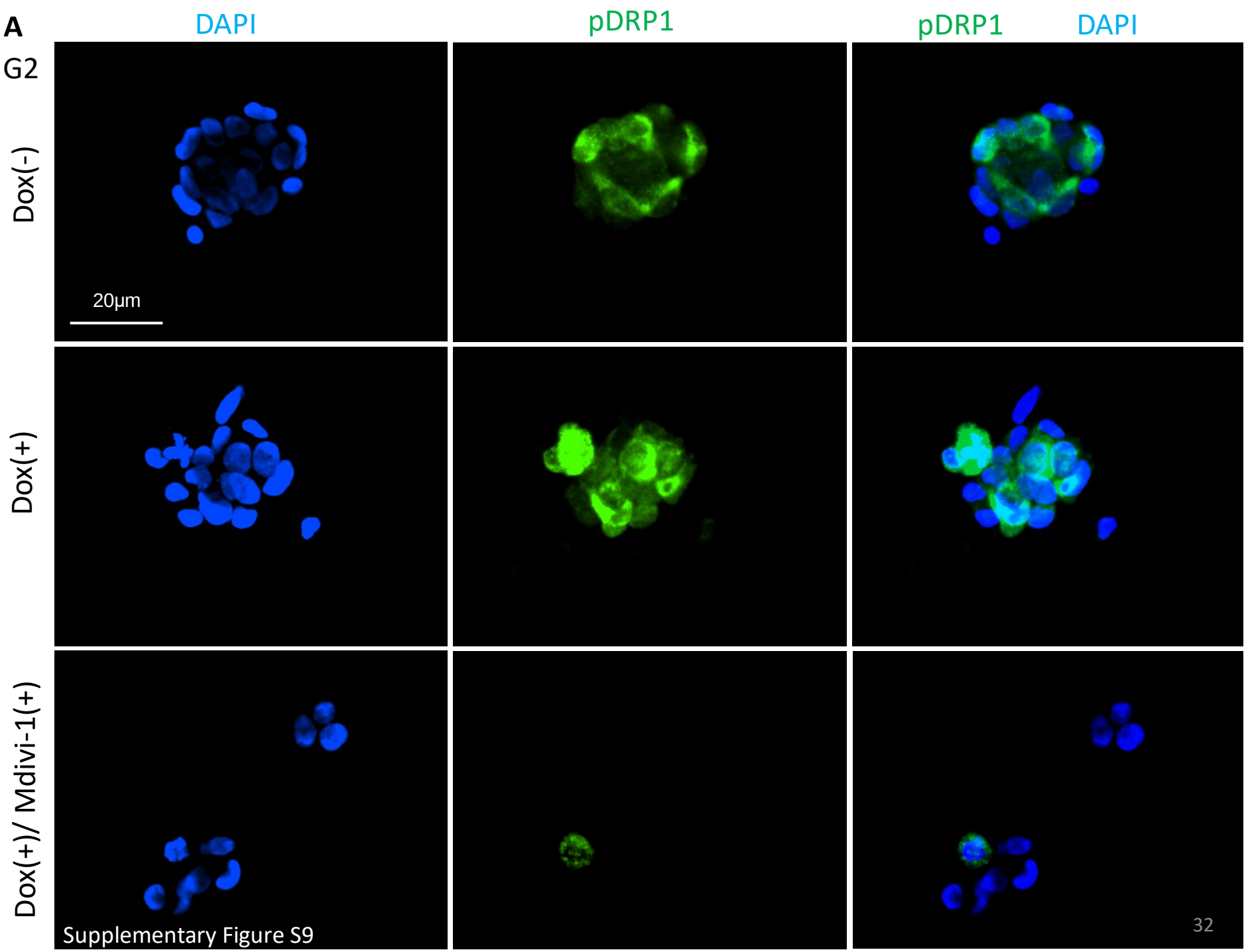

Supplementary Figure S9

B

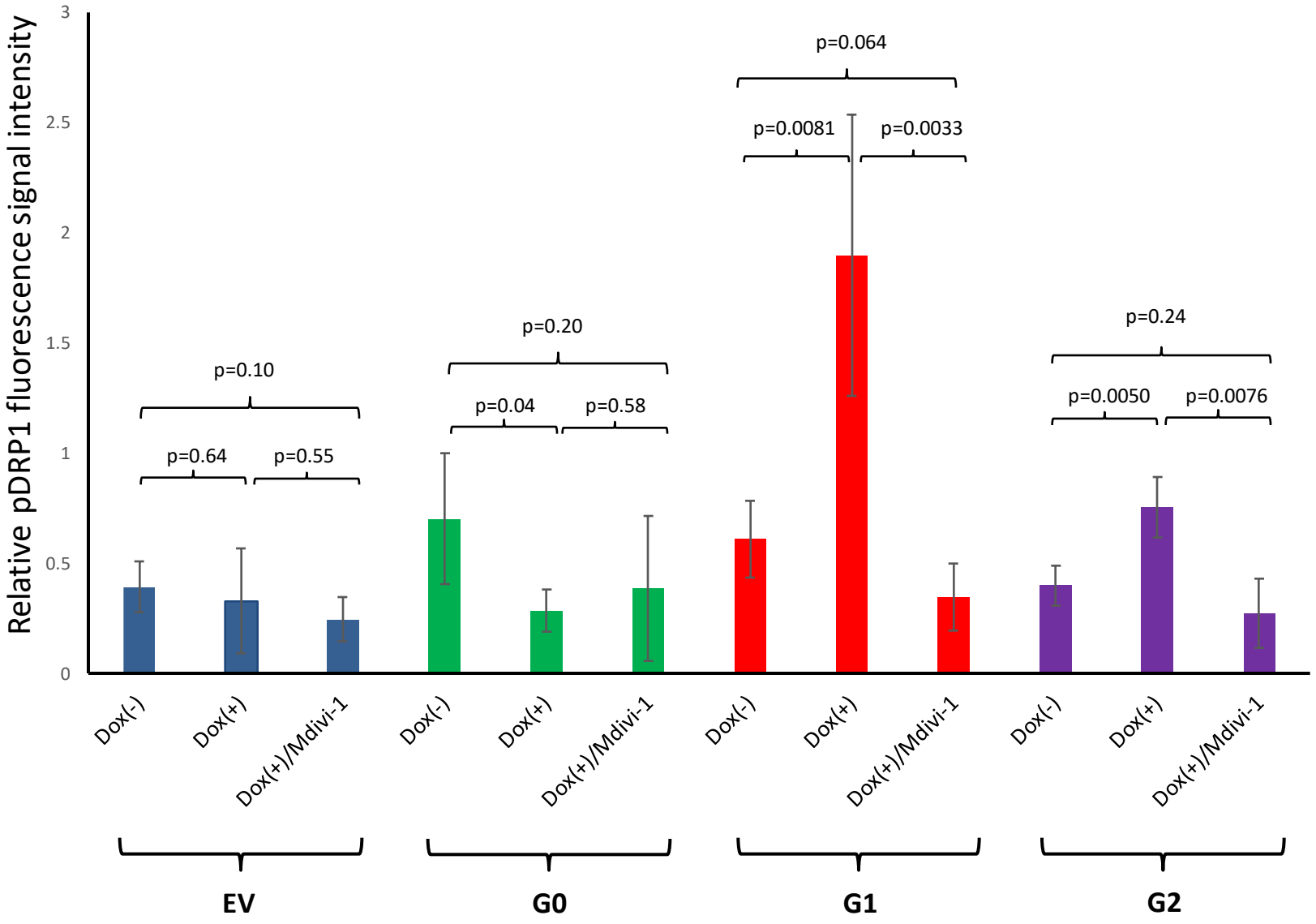

Supplementary Figure S9

Supplementary Figure S9. Phospho-DRP1 at Ser 616 (pDRP1) responses to *APOL1* overexpression and Mdivi-1 rescue.

A) HEK293 Tet-on EV, G0, G1, or G2 cells were grown without (-) Dox and without Mdivi-1, with Dox (+) only, and with (+) Dox and Mdivi-1 for 24 hr in full DMEM growth media. The final concentrations for Dox and Mdivi-1 were 10ng/ml and 50µM, respectively. After washing with PBS, cells were fixed with 4% paraformaldehyde and washed with PBS, then stained for pDRP1 (green) and counterstained with DAPI (blue).

B) For EV cells, Dox and Mdivi-1 did not change the pDRP1 signal intensity. For G0 cells, pDRP1 was down-regulated by overexpression of APOL1 G0; however, Mdivi-1 did not further inhibit pDRP1 levels. In contrast, Dox-induced *APOL1* G1 and G2 overexpression increased pDRP1 levels, and addition of Mdivi-1 reduced pDRP1 levels. The phospho-DRP1 signal intensity was normalized by DAPI in four independent wells of EV, G0, G1 or G2 cells without Dox and Mdivi-1, with Dox only, and with both Dox and Mdivi-1.

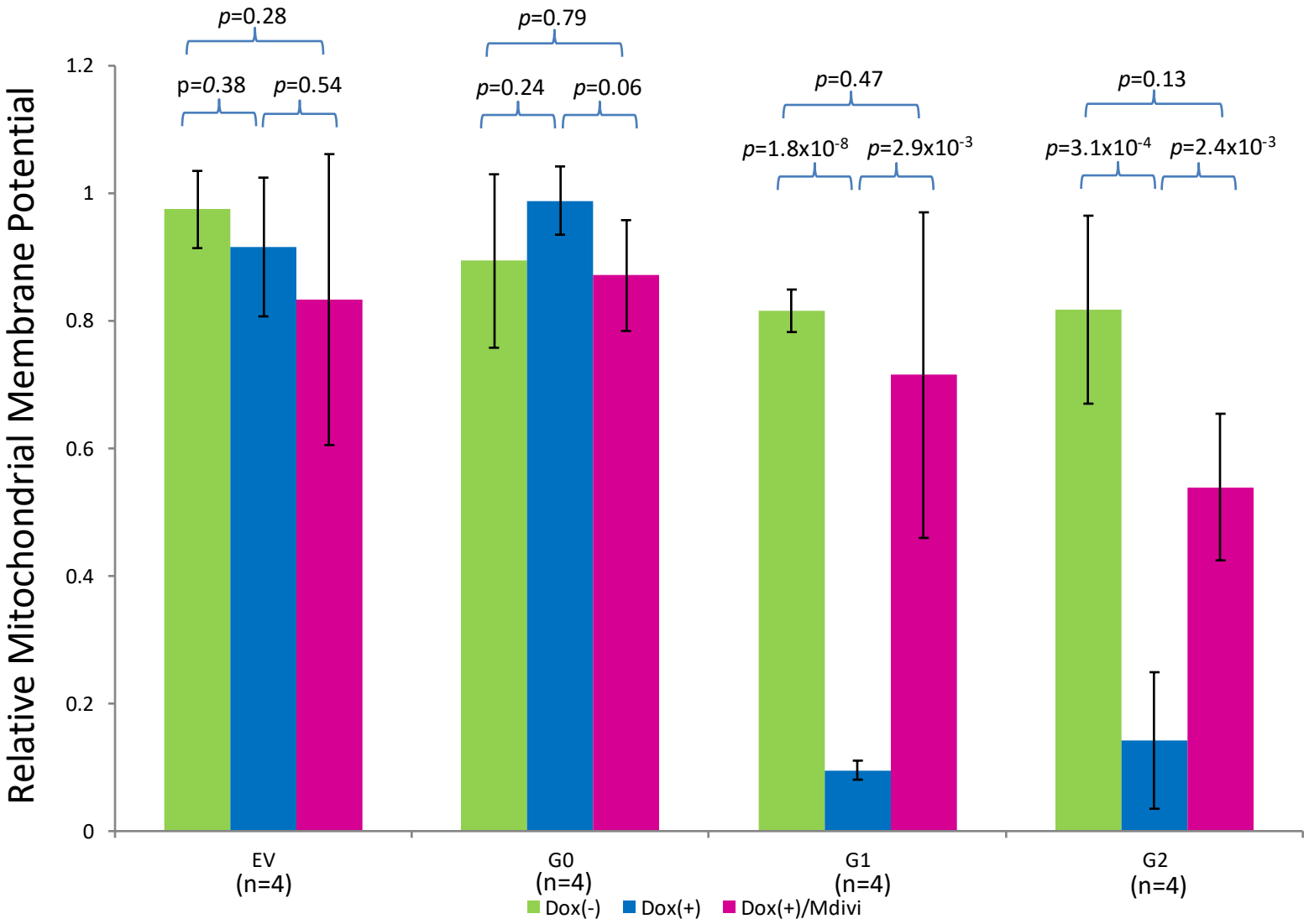

Supplemental Figure S10

Supplementary Figure S10. Relative mitochondrial membrane potential was reduced in Dox-induced HEK293 Tet-on *APOL1* G1 and G2 cells and rescued by Mdivi-1. HEK293 Tet-on EV, G0, G1, or G2 cells were grown without (-) Dox and without Mdivi-1, with Dox (+) only, and with both Dox (+)/ Mdivi-1 (+) for 16 hr in full DMEM media in a 24-well plate. The final Dox concentrations were 10, 10, 5, 10 ng/ml for EV, G0, G1, and G2 cells, respectively; these conditions maintained cell viability and produced comparable APOL1 overexpression levels in G0, G1, and G2 cells. In Dox (+)/Mdivi-1 (+) cells, the final concentration for Mdivi-1 was 50 μM. Cells were subsequently incubated with 50 nM mitotracker green (Invitrogen) and 10 nM TMRE (Tetramethylrhodamine ethyl ester, Invitrogen), a live cell fluorescence marker of mitochondrial membrane potential, for 30 min. Fluorescence signals of TMRE and mitotracker green were captured using an Olympus IX71 fluorescence microscope on four different wells of HEK293 Tet-on EV, G0, G1 and G2 cells. Fluorescence signals were measured by Image J (http://imagej.nih.gov/ij/). Pair-wise t-tests were performed to estimate the difference in relative mitochondrial membrane potential, defined as TMRE/mitotracker ratio, across cells without (-) Dox and without Mdivi-1, with Dox (+) only, and with both Dox (+) / Mdivi-1 (+) in each of genotype HEK293 cells. Reduced relative mitochondrial membrane potential was observed in Dox-induced HEK293 Tet-on G1 and G2 cells, an effect partially restored by Mdivi-1.

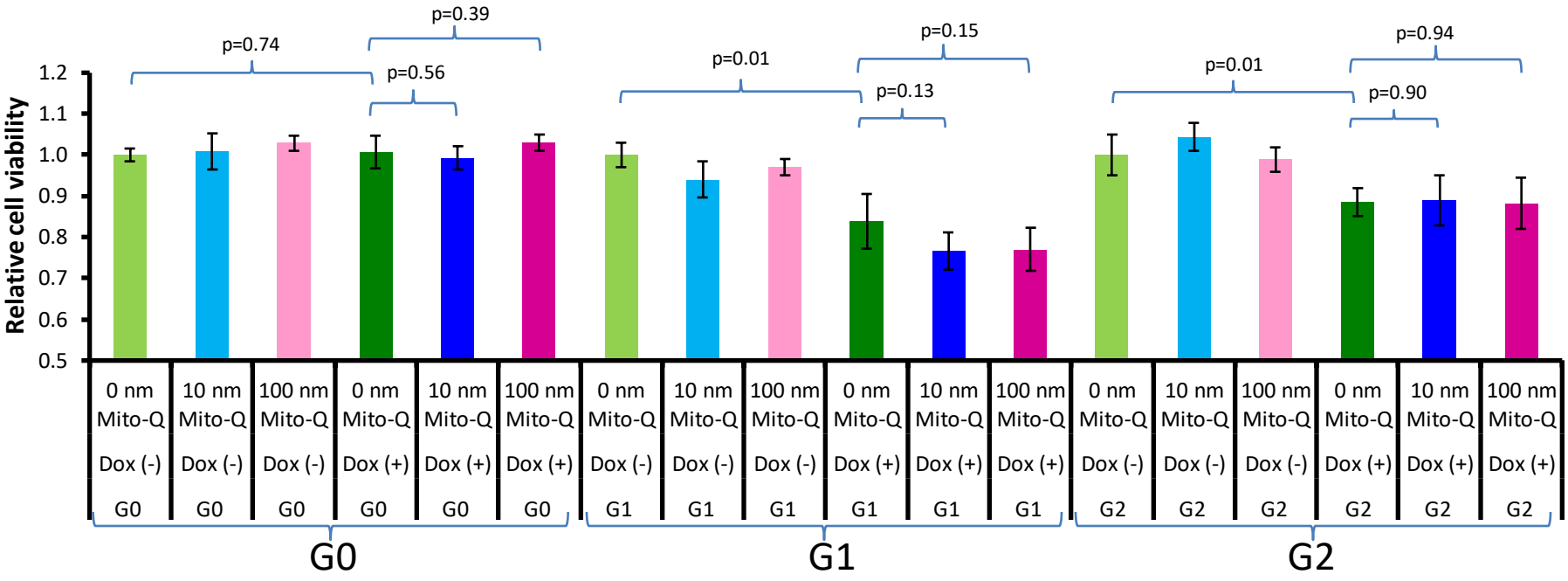

Supplementary Figure S11. Cell viability in HEK293 Tet-on cells overexpressing *APOL1* G0, G1 and G2 when treated with Mito-Q. Final concentrations of Mito-Q (0, 10nm, and 100nm) were applied to HEK293 G0, G1, and G2 cells without (-) and with (+) 10ng/ml Dox induction for 24 hr (n=4 for each treatment group). Dox induction did not impact cell viability in HEK293 Tet-on G0 cells, while G1 and G2 cells had reduced viability after 24 hr Dox induction (p=0.01 and 0.01, respectively). Mito-Q did not affect cell viability in HEK293 Tet-on G0, G1, and G2 cells without Dox induction. Mito-Q (10nm or 100nm) did not restore cell viability in Dox-induced G1 and G2 cells compared to those without Mito-Q.

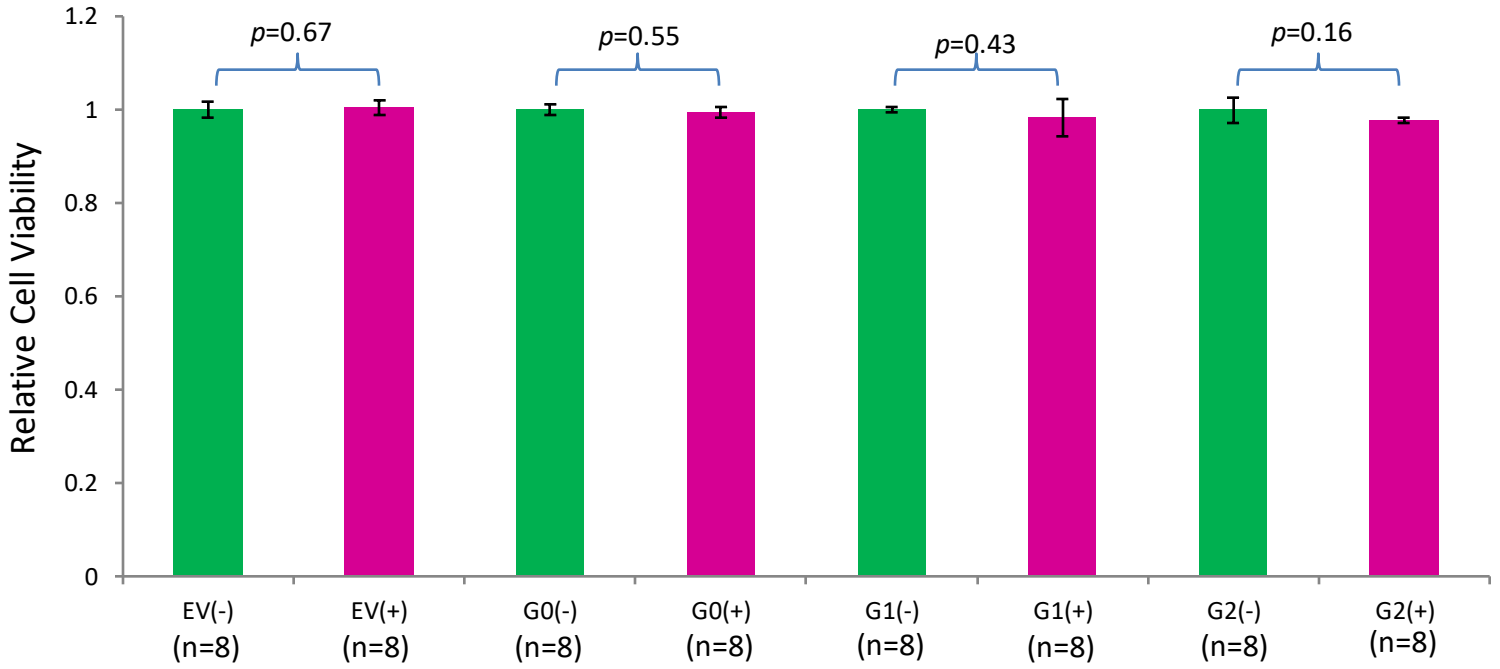

Supplementary Figure S12. Quantitative cell viability in HEK293 Tet-on EV, G0, G1, or G2 cells after 16 hr Dox induction. HEK293 Tet-on empty pTRE2hyg vector (EV), *APOL1* G0, G1, and G2 cells were seeded on three 96-well plates at a density of 20,000/well. Cells were induced (+) for 16 hr with final Dox concentrations of 10, 10, 5, 10 ng/ml for EV, G0, G1, and G2 cells, respectively, in complete DMEM media. Non-induced (-) cells were incubated with corresponding DMEM media without Dox. Cell viability was measured using the Cytotox 96 LDH viability assay kit (Promega, Madison, WI) per manufacturer instructions. Each cell line (with and without Dox induction) was measured independently in 8 wells, with values expressed as mean ± SD on the bar graph. One hundred percent cell viability was defined as "1".

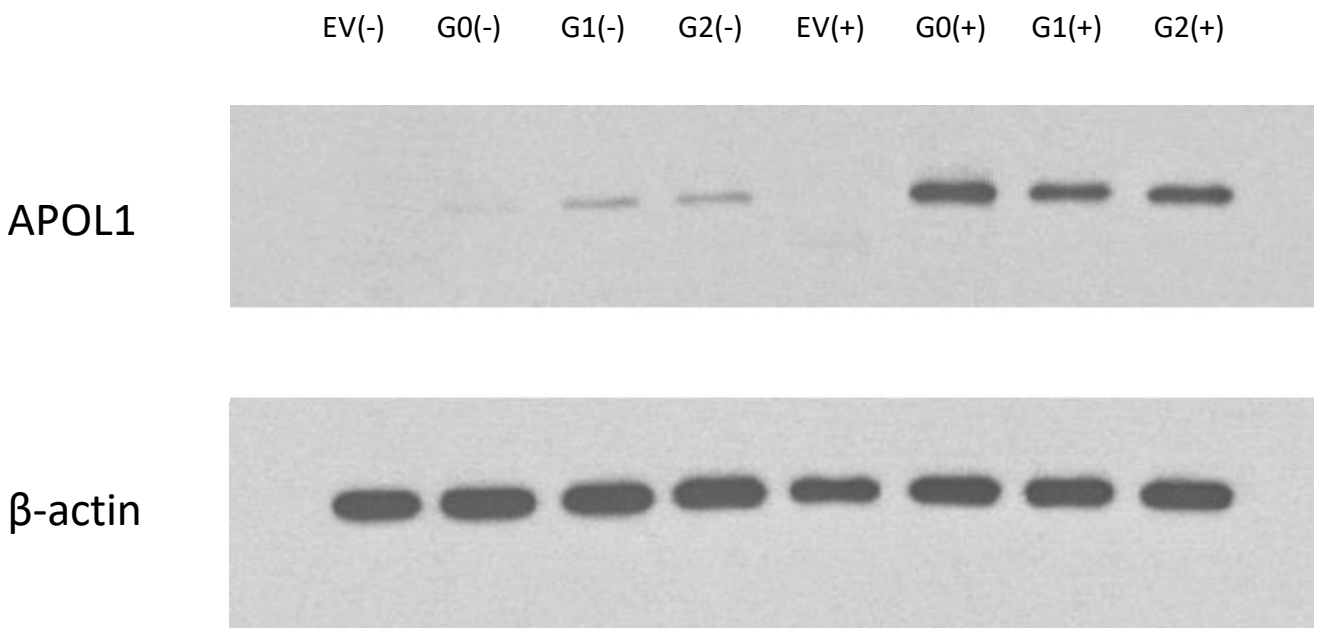

Supplementary Figure S13. Relative APOL1 expression levels were comparable in HEK293 Tet-on cells with Dox induction for 16 hr. Cells were induced (+) to express APOL1 for 16 hr with final Dox concentrations of 10, 10, 5, 10 ng/ml for EV, G0, G1, and G2 cells, respectively, in complete DMEM media. Non-induced (-) cells were incubated with corresponding DMEM media without Dox. Four ug of total cell lysate protein was loaded onto a 4-20% SDS-PAGE gel and probed with APOL1 (Abcam) and β-actin antibodies. EV cells did not express APOL1 with or without Dox induction. HEK293 Tet-on APOL1 G0, G1, and G2 cells expressed similarly increased levels of APOL1 with Dox induction. Trace amounts of APOL1 were present in HEK293 Tet-on cells without Dox induction. The data are representative of three trials of immunoblot with similar results.

Supplementary Table S1. Top 20 most differentially expressed pathways (1060 down-regulated and 1212 upregulated) after poly IC in the 50 African American primary renal PTC lines using Cytoscape BiNGO

Pattern	GO-ID	Description	x	n	X	N	p-value	corr p-value
Down-regulation	5737	cytoplasm	615	7622	926	17732	2.7398E-49	1.4872E-45
	44444	cytoplasmic part	460	5135	926	17732	1.9403E-42	5.2661E-39
	5739	mitochondrion	169	1272	926	17732	7.3149E-31	1.3235E-27
	9987	cellular process	648	9340	926	17732	2.5635E-28	3.4787E-25
	44281	small molecule metabolic process	170	1365	926	17732	1.1142E-27	1.2095E-24
	44424	intracellular part	718	10921	926	17732	1.7069E-26	1.5442E-23
	8152	metabolic process	461	5941	926	17732	6.5763E-26	5.0995E-23
	5622	intracellular	731	11275	926	17732	2.2566E-25	1.5311E-22
	44237	cellular metabolic process	401	4975	926	17732	1.4551E-24	8.7758E-22
	44429	mitochondrial part	99	610	926	17732	1.8018E-24	9.7257E-22
	6082	organic acid metabolic process	95	569	926	17732	1.9709E-24	9.7257E-22
	43436	oxoacid metabolic process	94	562	926	17732	3.0712E-24	1.2823E-21
	19752	carboxylic acid metabolic process	94	562	926	17732	3.0712E-24	1.2823E-21
	5829	cytosol	158	1313	926	17732	4.7437E-24	1.8392E-21
	42180	cellular ketone metabolic process	94	576	926	17732	1.9342E-23	6.9993E-21
	9058	biosynthetic process	188	1792	926	17732	1.2709E-21	4.3114E-19
	44249	cellular biosynthetic process	177	1682	926	17732	1.9279E-20	6.1555E-18
	44238	primary metabolic process	402	5273	926	17732	9.3472E-20	2.8187E-17
	3824	catalytic activity	384	5083	926	17732	7.4747E-18	2.1354E-15
	44283	small molecule biosynthetic process	70	444	926	17732	7.4044E-17	2.0096E-14
Up-regulation	2376	immune system process	176	950	880	17773	6.3121E-56	3.288E-52
	6955	immune response	128	619	880	17773	1.4946E-45	3.8927E-42
	2682	regulation of immune system process	81	437	880	17773	1.8267E-25	3.1718E-22
	6952	defense response	97	624	880	17773	2.7587E-24	3.5925E-21
	50896	response to stimulus	296	3635	880	17773	4.8708E-21	5.0744E-18
	6950	response to stress	177	1780	880	17773	2.369E-20	2.0567E-17
	48002	antigen processing and presentation of peptide antigen	18	24	880	17773	2.7484E-19	2.0452E-16
	2474	antigen processing and presentation of peptide antigen via MHC class I	15	16	880	17773	3.5901E-19	2.3376E-16
	51704	multi-organism process	100	786	880	17773	1.6423E-18	9.5055E-16
	45653	negative regulation of megakaryocyte differentiation	14	15	880	17773	6.9032E-18	3.4344E-15
	9607	response to biotic stimulus	70	448	880	17773	7.2525E-18	3.4344E-15
	19882	antigen processing and presentation	25	59	880	17773	1.0164E-17	4.412E-15
	48518	positive regulation of biological process	196	2209	880	17773	4.7038E-17	1.8848E-14
	51707	response to other organism	60	357	880	17773	5.5024E-17	2.0473E-14
	9615	response to virus	36	142	880	17773	2.1227E-16	7.3714E-14
	48583	regulation of response to stimulus	74	526	880	17773	2.9876E-16	9.7264E-14
	48519	negative regulation of biological process	181	2036	880	17773	9.0235E-16	2.7649E-13
	7165	signal transduction	171	1891	880	17773	1.454E-15	4.2077E-13
	48522	positive regulation of cellular process	178	2004	880	17773	1.8286E-15	5.0132E-13
	51239	regulation of multicellular organismal process	115	1080	880	17773	2.6999E-15	7.0318E-13

Note: x, number of gene IDs identified in the designated pathway among input gene IDs; X, number of input gene IDs selected by BiNGO; n, number of known gene IDs in the designated pathway; N, number of background gene IDs selected from the GO pool by BiNGO. Replicated pathways in the subsequent Ingenuity pathway analysis are shown in red. P-values are shown as scientific E notation (e.g. 2.00E-5 is equivalent to 2.00×10^{-5}) hereafter throughout the supplementary tables.

Supplementary Table S2A. Top canonical pathways detected based on the most down-regulated genes by poly IC in 50 primary African American renal PTC lines using Ingenuity Pathway Analysis

Ingenuity Canonical Pathway	p-value	Molecules
Superoxide Radicals Degradation	1.29E-03	CAT,NQO1
Inhibition of Angiogenesis by TSP1	1.38E-03	SDC2,GUCY1B3,SDC1
Oleate Biosynthesis II (Animals)	2.06E-03	SCD5,SCD
Mitochondrial Dysfunction	4.09E-03	UCP2,CAT,BCL2,GSR,ACO1
Urate Biosynthesis/Inosine 5'-phosphate Degradation	4.09E-03	IMPDH2,AOX1

Replicated pathways in Supplementary Table S1 are shown in red.

Supplementary Table S2B. Top canonical pathways detected based on the most up-regulated genes by poly IC in 50 primary African American renal PTC lines using Ingenuity Pathway Analysis

Ingenuity Canonical Pathway	p-value	Molecules
Interferon Signaling	2.14E-19	IRF1,OAS1,JAK2,IFITM1,IFNAR2,IFNGR2,IFIT3,STAT2,IFI6,TAP1,IFIT1,STAT1,ISG15,IFITM2,IFI35,MX1,PSMB8
Communication between Innate and Adaptive Immune Cells	1.12E-15	CCL3,HLA-E,CSF2,CCL5,IL1B,HLA-G,CD40,IL6,HLA-F,TNFSF13,CXCL8,HLA-A,IL1RN,TLR3,TNF,IL1A,HLA-C,HLA-B,TLR2
Antigen Presentation Pathway	4.23E-13	HLA-E,CD74,HLA-G,TAP1,TAPBP,HLA-F,HLA-A,TAP2,HLA-C,HLA-B,MR1,PSMB9,PSMB8
Role of Pattern Recognition Receptors in Recognition of Bacteria and Viruses	7.82E-13	EIF2AK2,OAS1,CSF2,MYD88,C3,CCL5,IL1B,CASP1,OAS2,DDX58,IL6,CXCL8,NFKB2,IRF7,TLR3,TNF,OAS3,IFIH1,IL1A,TLR2,PTX3
Granulocyte Adhesion and Diapedesis	1.30E-12	ICAM2,CCL3,CCL28,CCL5,IL1B,CCL20,CCL3L1,CXCL2,CXCL8,CX3CL1,CXCL6,TNFRSF11B,IL1RN,TNF,CCL2,IL1A,CXCL1,CXCL16,CSF3,SDC4,CXCL5,ICAM1,MMP1

Replicated pathways in Supplementary Table S1 are shown in red.

Supplementary Table S3. Expression primer sequence information

Expression primer ID	Sequence (5' to 3')	Amplicon size
APOL1_F	TGATAATGAGGCCTGGAACG	141bp
APOL1_R	TACTGCTGGCCTTT ATCGTG	
18s_F	ATCAACTTTCGATGGTAGTCG	109bp
18s_R	TCCTTGGATGTGGTAGCCG	
ACTB_F	CACCATTGGCAATGAGCGGTTC	135bp
ACTB_R	AGGTCTTTGCGGATGTCCACGT	

Primer sets were designed across different exons of indicated transcripts based on UCSC Genome Bioinformatics (http://genome.ucsc.edu/). Each amplicon size was verified by agarose gel and UCSC in-silico PCR. Dissociation curve analysis confirmed the specificity of SybrGreen RT-PCR.

Supplementary Table S4. Primary antibodies used in immunoblot and immunofluorescence

Antibody	Vendor	Catalog #	Host species	Dilution
Immunoblot				
APOL1	Abcam	Ab108315	rabbit	1:1,000
APOL1	Sigma	HPA01885	rabbit	1:1,000
BAK1	Santa Cruz	Sc-517390	mouse	1:1,000
DRP1	Abcam	ab156951	mouse	1:1,000
Fis1	Abcam	ab71498	rabbit	1:1,000
Opa1	Abcam	ab42364	rabbit	1:1,000
MFN1	Abcam	ab57602	mouse	1:1,000
MFN2	Abcam	ab56889	mouse	1:1,000
COXIV	Cell Signaling	4850	rabbit	1:1,000
β-actin	Sigma	A5441	mouse	1:10,000
Immunofluorescence				
APOL1	Abcam	Ab108315	rabbit	1:500
BAK1	Cell Signaling	12105S	rabbit	1:200
BAK1	Santa Cruz	Sc-517390	mouse	1:100
ATP5A1	Invitrogen	439800	mouse	1,000
WT1	Thermo	ms-1837-s	mouse	1:100
Podocalyxin	R&D systems	MAB1658	mouse	1:50
CD31	BD BioSciences	550389	mouse	1:25
DPP4/CD26	BD BioSciences	555435	mouse	1:100
αSMA	Abcam	Ab7817	mouse	1:50
pDRP1(Ser616)	Cell Signaling	3455S	rabbit	1:400